Exploring the Surface of Titan

by

R. D. Lorenz

A thesis submitted in partial fulfilment of the requirements of the degree of Doctor of Philosophy at the University of Kent at Canterbury

University of Kent at Canterbury
United Kingdom

July 1994

Chapter 7

Impact Measurements

'Why, then the world's mine oyster, which I with sword will open'
William Shakespeare
The Merry Wives of Windsor

'For my part, I travel not to go anywhere, but to go. I travel for travel's sake: the great affair is to move, to feel the needs and hitches of this life more nearly, to come down from this feather-bed of civilisation and find the globe granite underfoot and strewn with cutting flints'
Robert Louis Stevenson
Travelling Upon a Donkey in the Cevennes

7.1 Introduction

The assessment and Phase A studies both identified impact accelerometry as a useful surface measurement, in part because of the assumed presence of accelerometers for entry dynamics measurements. Both the HASI and SSP experiments carry accelerometers, although little in the way of preparatory theoretical or experimental work was done on assessing what science could be determined from the measurements, with 'probe response to impact' being the stated measurement objective. In part, this is due to lack of manpower (actual development of the instrumentation being perceived as more important than considering its interpretation) and in part due to the paucity of information on the structural properties of the final probe design.

The present author played a large role in predicting the expected impact profiles for both solid and liquid impacts, and specifying the required measurement ranges and sampling frequencies for both the SSP and HASI accelerometers. As mentioned in the previous chapter, it was decided to optimise the SSP accelerometers for an impact on a solid, with those on HASI optimised for impact (and post-impact) dynamics for liquid surfaces.

7.2 Review

As described in Lorenz (1994b) the landing loads for spacecraft on liquid surfaces is fairly well-documented as a result of work on the Mercury, Gemini and Apollo programmes. A fairly simple 'added mass' method can be used to compute decelerations; this method is also used for evaluating ditching loads on aircraft (Leigh, 1988).

Literature on spacecraft impact loads on solid surfaces is rather more scattered: a list of relevant references may be found in Lorenz (1994b). The subject is further complicated by the large amount of work on penetrators (i.e. long, slender vehicles) designed to penetrate a significant distance into the surface material. The dynamics of such vehicles are complicated, since they are acted upon by frictional forces along their length as well as by forces at their tip. Although empirical relations (Young, 1967) exist for predicting their depth of penetration and deceleration loads, the deceleration profiles are complicated, even for uniform surface materials.

The influence of a 'penetrator' mindset is evident in the evolution of the SSP accelerometers. This is perhaps unsurprising, since before the ESA M1 mission selection of Huygens, effort at UKC had been focussed on an asteroid mission, Vesta. When Vesta (which featured a number of asteroid penetrators) was not selected, efforts to utilise or 'recycle' development work on Vesta instruments (accelerometers and thermal properties) led to these instruments playing a large role in SSP.

7.3 ACC-E

Originally the concept for an impact accelerometer on SSP was to place a piezoelectric accelerometer on a short stub (on which was also mounted the XRF subsystem). As the SSP and probe design evolved in Phase B1, with a glass-fibre top-hat and thin fore-dome, a 'pylon' was envisaged - a slender but stiff structure to put the accelerometer as far forward as possible, yet have it as strongly-coupled as possible to the experiment platform.

In Phase B2, in summer 1991, the author (then part of the ESA project team) was asked to examine whether this location and mounting was suitable. I found (R Lorenz, unpublished memo 24/9/91) that the location was acceptable, but that the transducer was inappropriate. Ultimately it is force that is the desired measurement, since it is this quantity (an 'effort' variable in transducer theory) which is generated by the surface material. Usually, in a rigid body such as a penetrator, this force produces an acceleration (a 'flow' variable in transducer theory), with the two quantities related by Newton's Second Law.

However, the acceleration of the pylon does not depend only on the soil force acting on it, but also due to the force at its mounting on the experiment platform. While in shape the pylon may resemble a penetrator, in dynamic terms it does not. If the pylon were perfectly rigid, the accelerometer could equally well (and more safely) be put at its base, near the

experiment platform, although both there and in its original location it would be susceptible to structural oscillations.

Thus, to eliminate these uncertainties in dynamics, it was proposed (Lorenz 24/9/91) to use a force transducer on the tip of the pylon, thereby measuring the force directly. A force measurement at the tip helpfully eliminates the effect of frictional forces along the pylon's length.

In order to minimise the changes to the SSP electronics design, a piezoelectric force sensor was suggested (strain gauges may have worked, although it was not certain that their bandwidth would have been adequate). Commercial force washers were expensive and presented some materials compatibility problems: it should be remembered that low outgassing, coupled with operation at cryogenic temperatures, was required. Thus it was decided to develop the transducer at UKC.

The initial development configuration used a piezoelectric disc (made of Lead Zirconate Titanate - PZT) sandwiched between two brass screw fittings, with the assembly held together with an epoxy adhesive. The brass screw fittings allowed experimental penetrator tips (conical and hemispherical) to be attached, and different pylons (kevlar- or carbon-reinforced plastic tubes, of 8 and 14mm diameters) to be used.

Signals from the transducer were amplified and passed to a home-made A/D converter, sampled by a BBC microcmputer (the BBC's internal ADC was too slow). Data was extremely noisy, but it was determined that the hemispherical tip gave a better (stronger) signal, with less structural ringing.

It was also noted, during the many breakages of the transducer, that a design held together with adhesive was not adequately robust. Thus the second generation of designs had a PZT washer as the sensing element, with the tip held onto the base by a bolt. These tips were 28mm in diameter, and were made of steel. An innovation suggested by Z Krsynski was the incorporation of a small electrode on the PZT washer to allow stimulation of the sensor for in-flight health verification. Two heads were made, one with the PZT washer exposed, the other with a lip which restricted sideways movement (at the suggestion of Al Seiff). These two sensors gave much better results, when used with an improved PC-based data acquisition system, the SMU (Stimulus and Monitoring Unit).

Interestingly, by examining the Fourier transform of the sensor's response to hammer blows, it was possible to discriminate between a hammer tap on the apex and on the side of the sensor. These taps presumably excited different oscillation modes of the support pylon.

Assembly of the sensor with the lip was very difficult, and the device gave no performance improvement, so the unlipped design was adopted. The next and final step in the ACC-E's evolution (summarised in figure 6.1) was the scaling down and the substitution of materials to reduce mass. Scaling to 14mm diameter reduced the transducer's mass by a large factor (although by forcing the relative sizes of the stimulus and sense electrodes, it rather complicated the calibration of the sensor : see later). Also aluminium was used as the material for the support collar and pylon, and titanium for the penetrator head (which could suffer rough treatment during test and calibration). An additional design aspect was that the pylon was now mounted on the top hat, rather than directly on the experiment platform.

The detailed design of the ACC-E subsystem, and its calibration, is described in Lorenz et al. (1994). The following comments describe small changes since that paper was submitted.

First, as details of the electronics emerged from RAL, it was realised that the stimulator circuit which would allow in-flight health checks of the system itself needed protection from the possible high voltages developed during test or accident. Thus a large capacitance was put between the stimulus and ground lines: the effect of this is to effectively remove the charge generated across these electrodes by the transducer. Since this charge is coupled capacitively to the sense electrodes, the force-voltage characteristic of the transducer is affected.

Second, an improvement has been made in the absolute calibration. Under my direction, Mick Willett wrote a program (Willett, 1994) to simulate the force-time profile of an impact of a lump of material onto the ACC-E transducer. This allows the prediction of the peak force produced by the ACC-E calibration jig, if the material properties (Young's Modulus E) are known.However, the quoted values for this quantity vary (e.g. 7-70Mpa in the Southampton Engineering Data Book). Since the peak force is proportional (McCarty and Carden, 1962) to $E^{0.4}$, this leads to a 60% uncertainty in the value of the force produced by the jig.

However, since the program generates a force profile, as does the instrument, these profiles may be compared. The force profile (for the rubber impactor, dropped from position 4 on the

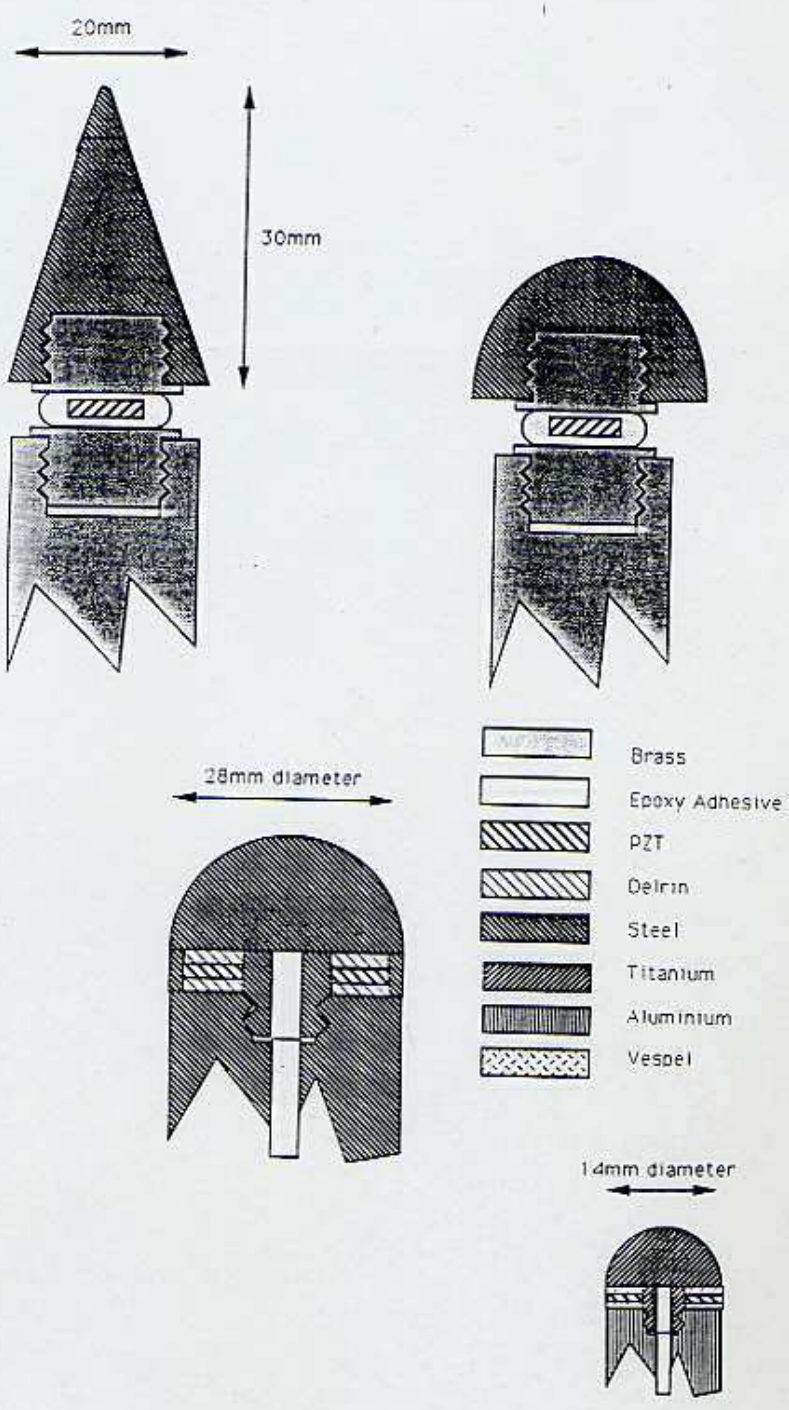

Figure 7.1 ACC-E Impact penetrometer evolution (top to bottom) First adhesive-bonded mockups, then large bolt/washer type, eventually scaled down to flight size

The intermediate stage and flight versions are seen in the TV programme (Balburnie 1994)

calibration jig i.e. impact speed 1.3 ms^{-1}) varies as a function of the assumed value of E (see figure 7.2)

The voltage as a function of time produced by the sensor (rubber impactor, position 4, with a 8nF capacitor across the sense and ground electrodes) is shown in figure 7.3. Two profiles are shown, indicating good reproducibility of the measurement. It is seen that the profile falls to zero is ~3.5 ms, corresponding closely with the curve in figure for E=20MPa. Further numerical experiments suggest that the range 18-20MPa is consistent, corresponding to values of the peak force of 142-148N.

Considering the various other uncertainties (including, significantly, the value of the capacitor used across the sensor during calibration) it is probable that the absolute calibration is good to ~5%.(Note that variations in force are measured to 8 bits using a logarithmic amplifier, so variations in force during the impact are measured to ~1%) Note that although a logarithmic amplifier is used, which allows a useful dynamic range with only an 8 bit measurement, with higher resolution sampling (e.g. 12 bit), a linear amplifier/filter, or perhaps even only a acapacitor, could be used. In the earlier stages of the ACC-E development (before much experimentation had been performed), the range of forces that should be measured was expected to be somewhat larger, so a logarithmic amplifier was selected. In much the same way, the use of titanium for the penetrator head is probably 'vestigial': the calibration stimuli envisaged used metal impactors which would have damaged an aluminium tip, but the teflon and rubber impactors now used could allow the substitution of aluminium for titanium, although the cost and mass saving would be very modest.

Some sample measurements for drops (5 ms^{-1}) of the sensor mounted on a 5kg steel mass by a small pylon into various materials are shown in figure 7.4 . The 'spiky' appearance of drops onto gravel may be noted. It is seen that the spacing between the peaks, and their magnitude depend the particle size (see also Newton, 1994 for discussion).Figure 7.5 illustrates this correlation.

7.4 Internal Accelerometry

Impact accelerometry in general, and the impact dynamics of the Huygens probe have been investigated in some detail by myself (Lorenz 1994b). Here I describe only the accelerometry instrumentation itself, and the work performed on interpretation methods.

The HASI accelerometers are the following:

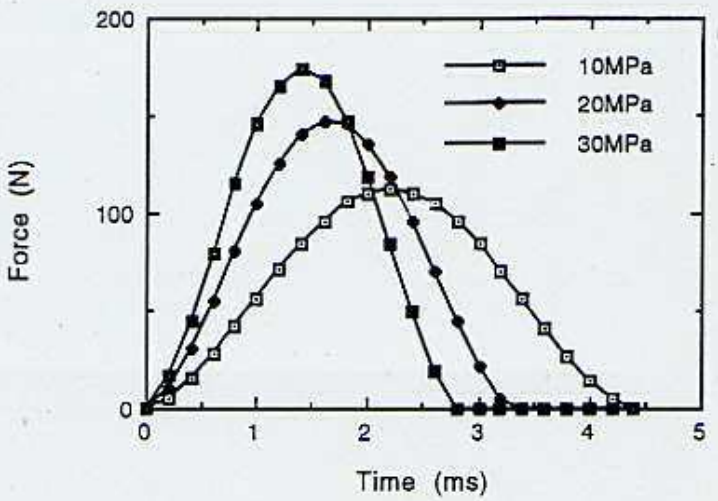

Figure 7.2 Theoretical force profiles produced by calibration jig with rubber impactor dropped from position 4, as a function of assumed rubber Young's modulus E

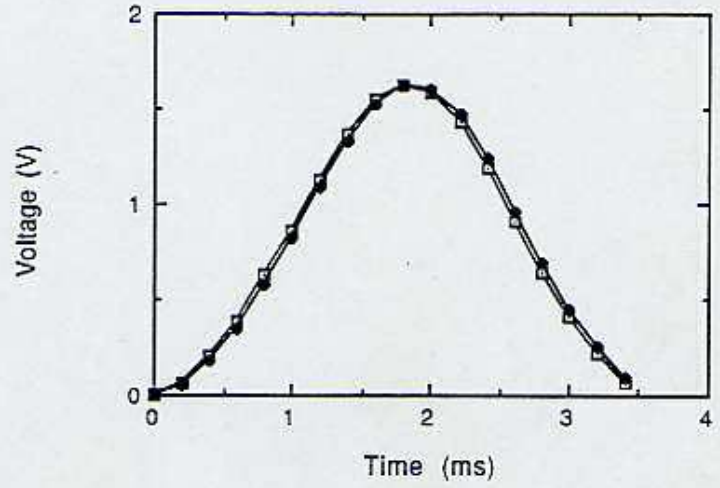

Figure 7.3 Transducer response to calibration force pulse (rubber impactor, position 4). Reproducibility is very good - the two examples here are virtually identical.

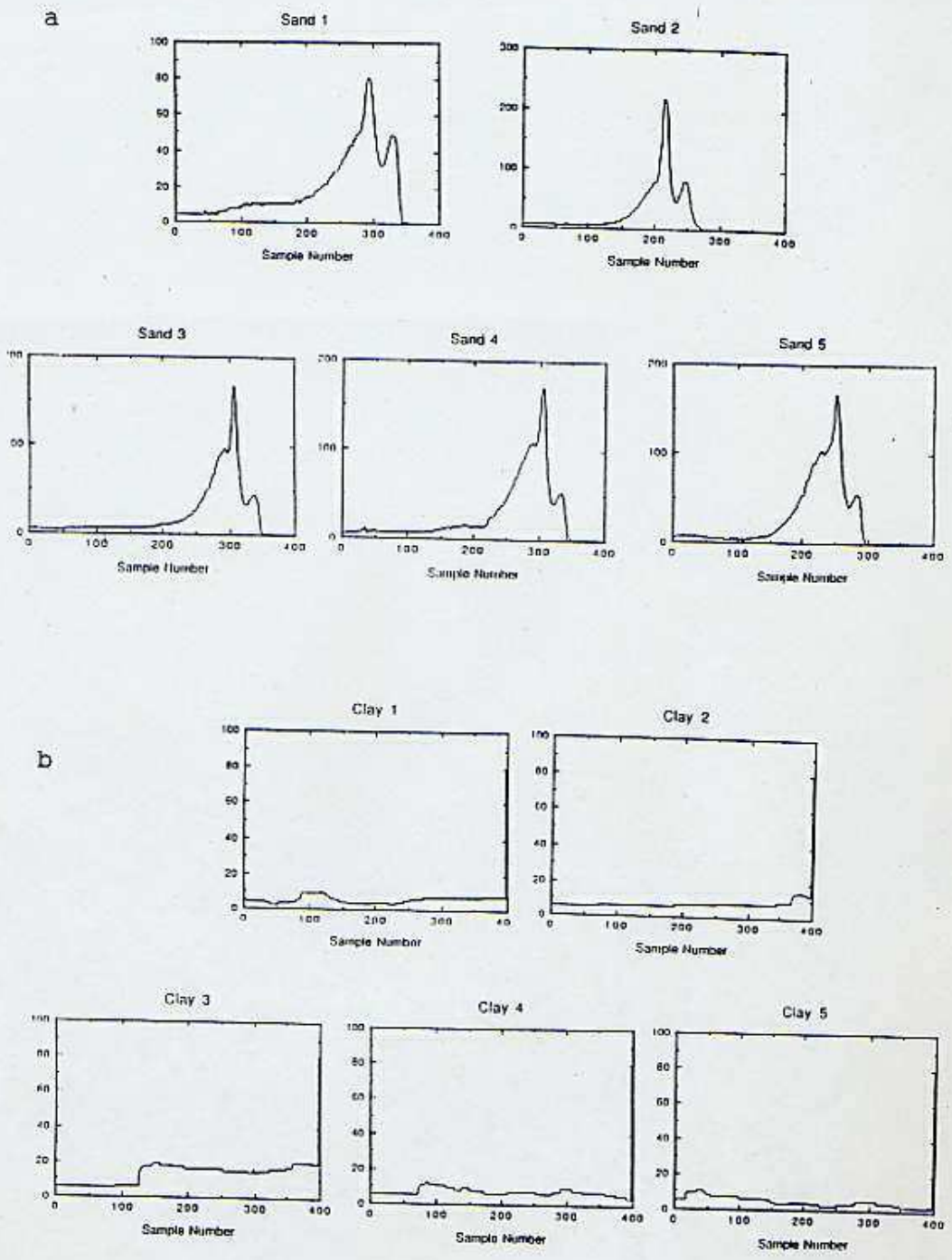

Figure 7.4 Penetrometer force profiles (arbitrary units) after pseudolog amplification. Abscissa is time, sampling at 10kHz, so sample 200=20ms. Profiles (a) for sand show a power-law rise, with a final wiggle due to impact of the drop weights. Profiles (b) show impacts into grey stone clay, and show a broadly constant resistance

c

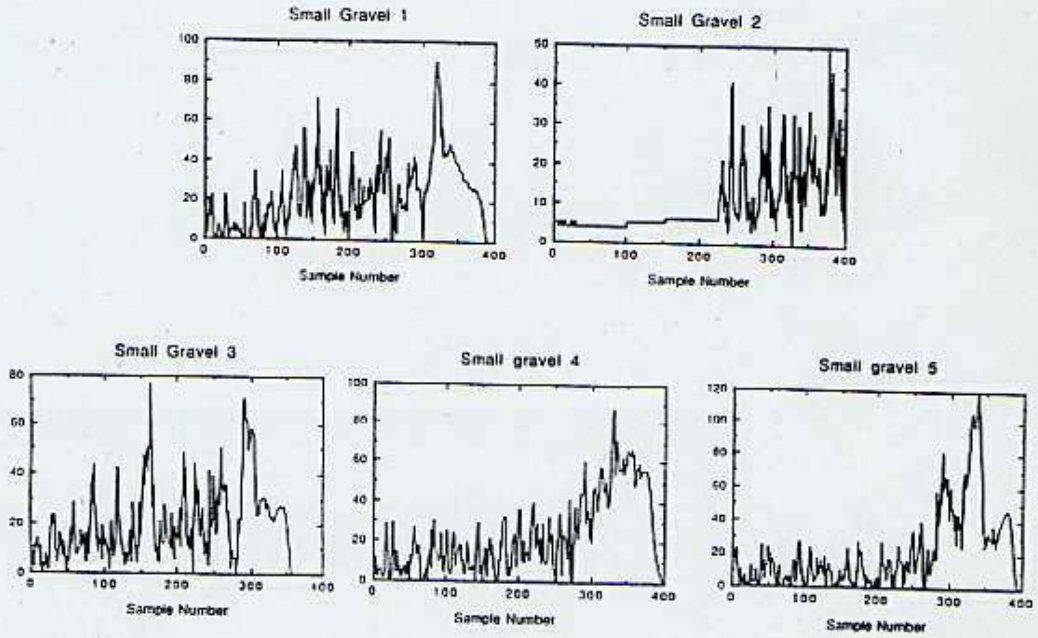

d

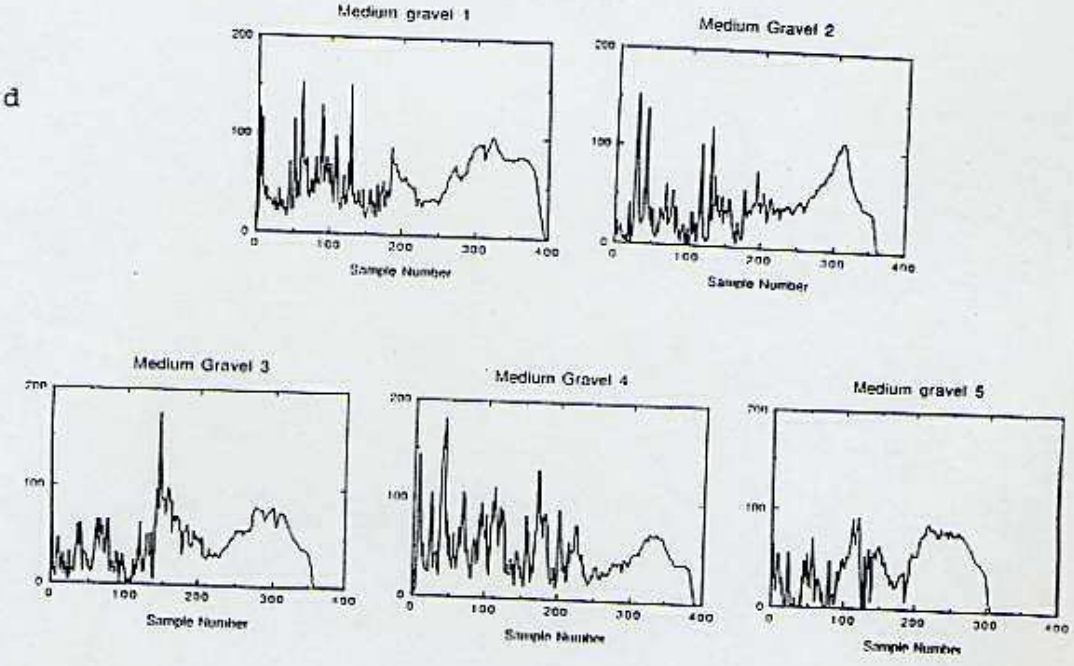

Figure 7.4 (continued) Axes as before. Drops (c) into fine gravel, with mean particle diameter of 8mm. Drops (d) are into coarser gravel, with mean diameter ~15mm - note the greater amplitude of the peaks, as well as their fewer number compared to (c). Broad bump at end of profile is 'bottoming out' of drop weights.

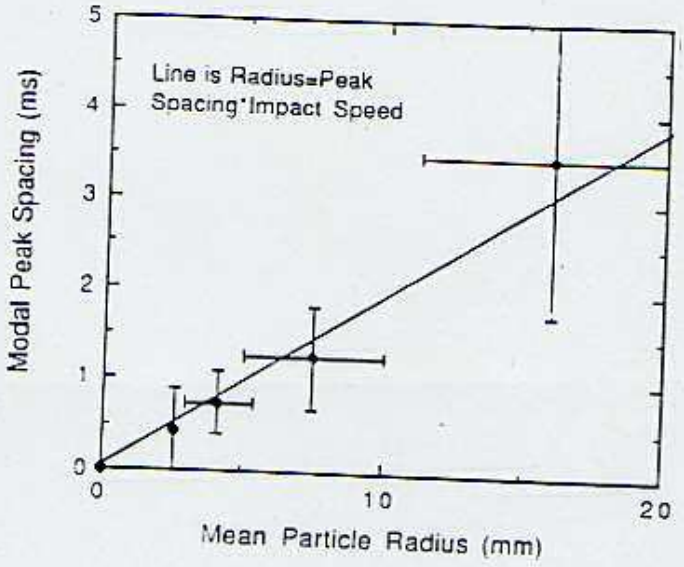

Figure 7.5 Correlation of Peak spacing and Particle size : Although statistics are poor, the peak spacing multiplied by the impact speed correlates well with the particle size

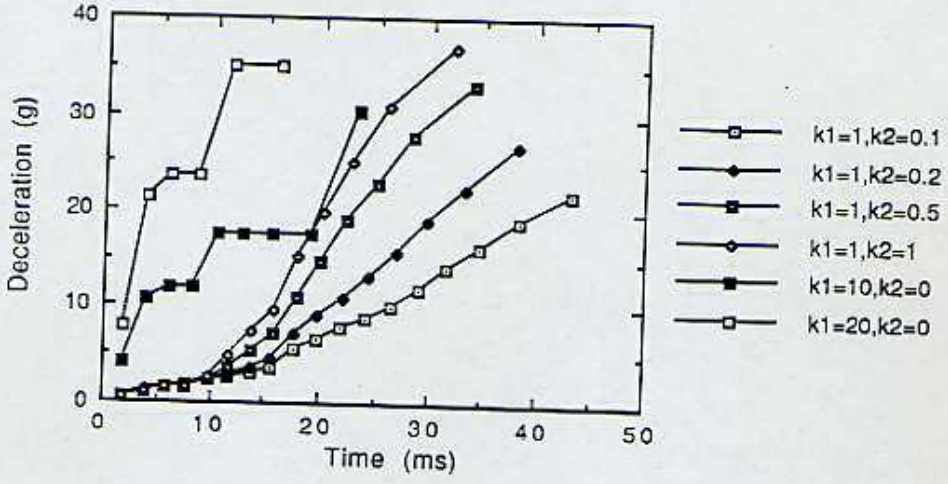

Figure 7.6 Probe Deceleration profiles for various solid materials : k1 is the bearing strength of the soil, k2 the subgrade modulus, or increase of bearing strength with depth. k1=20 corresponds to a sludge surface, k1=1,k2=0.2 corresponds to sand or regolith

1 Sunstrand QA-2000-030 electromagnetic servo accelerometer, mounted at the cg of the probe along the X axis (i.e. the spin axis of the probe, nominally vertical at impact).
3 Endevco 7264A-2000T piezoresistive accelerometers, also mounted at the probe cg, measuring in three orthogonal axes

The servo accelerometer is sensitive (few μg resolution) for entry measurements, but has a range of only 25g, and its bandwidth is limited (by the servo loop) to 100Hz. Thus the servo accelerometer is not used for impact measurements, as it would respond too slowly to impact accelerations.

The piezoresistive accelerometers are sampled during descent at 50 samples/second, with data averaged over 1 second intervals and telemetered. Near the surface, the measurement rate is increased to 400 samples/second along the X-axis, and 50 samples/second in the Y and Z axes to accurately characterise the splashdown and subsequent bobbing in the event of a liquid landing. These transducers are able to measure to ~2000g, but due to the configuration of the sampling electronics (designed to maximise entry sensitivity to give 50 mg resolution), their upper limit is 20g. Thus, the HASI sensor suite will characterise liquid impacts well (~10g), but do not have sufficient range to cover impacts on regolith or harder materials.

However, SSP carries an Endevco 2271A piezoelectric accelerometer, mounted on the SSPE box, about 25cm from the probe centre. This accelerometer is sampled at 500 samples/second, giving a good profile of both liquid and solid impacts, and allowing (hopefully) the identification and removal of features in the accelerometer profile due to structural oscillations of the probe.

Since this accelerometer is near the edge of the probe, angular accelerations at impact may give an additional component to this signal. Hopefully, however, combination of HASI and SSP ACC data, with that of SSP TIL, should allow the extraction of this component.

Interpretation of accelerometry relies on the ability to discriminate the effects of the mechanical properties of the probe on the accelerometer signal from the effects of the mechanical properties of the surface material. Thus knowledge is required of the effect of the coupling of soil mechanical properties to the probe (largely a problem of geometry - see section 7.2, and Lorenz 1994b) and the probe's response, which depends on the strength and stiffness of its structure.

The concept for interpretation of the probe response envisaged in the SSP proposal was to use a physical model of the probe, named DYN ('dynamic'), in drop tests. This would have

required flight-representative models of the main probe structural elements, such as the experiment platform and fore-dome. These would have been expensive to procure, and many of the drop tests would have been destructive (although it should be noted that the proposal was based on the Phase A design of the probe, which was somewhat more rigid than the eventual configuration - see chapter 5).

As the probe design evolved, it emerged that the fore-dome would not sustain a large load: thus the main load path for loads due to the soil on the bottom of the probe at impact would be through the equipment boxes on the underside of the experiment platofrm, rather than through the fore-dome and its attachment points. Obtaining or building boxes with flight-representative structural characteristics (which would require the cooperation of experiment teams and the various probe subsystem contractors - not just the inner structure subsystem contractor CASA, who supply the fore dome and experiment platform) would be impracticably expensive.

Thus a numeric model was set up, modelling the probe boxes as a set of (non-linear) springs, making engineering guesses as to the structural properties of the various boxes. The model is described in detail in Lorenz (1994b) Setting up the model with realistic parameters relied on the availability of engineering drawings of the GCMS, ACP and SSP structures, and that of the large PCDU box; the author's close association with the project team was useful in obtaining these drawings. In the (unlikely) event of test data, or spare models of these boxes, becoming available, it will be useful to update the model parameters.

The model also includes the load path due to the fore dome. A linear law was assumed, first for simplicity, and second, model test data on the Apollo heat shield structure (Stubbs, 1967) indicated a broadly linear force-deformation characteristic. It was further foumd, during numerical experiments with the model (Appendix in Lorenz 1994b) that the accceleration profiles are relatively insensitive to realistic variations in the force-deformation characteristic of the fore-dome.

Acceleration profiles are indicated in figure 7.6.

7.5 Analysis and Interpretation

The Huygens instruments will provide acceleration or force profiles as a function of time during the impact event.

The Surveyor landing loads were investigated to deduce soil parameters by generating simulated force profiles for different soil parameters and comparing visually with those actually measured (Sperling and Galba 1967). Such a method is probably the most appropriate for Huygens, since there is only one set of data to examine, and depending on the other mission results, an appropriate effort invested in analysing the data. In principle a small catalogue, either on hard copy or in software form, could be built up and compared with the flight dataset as soon as it is received (assuming, of course, that Huygens survives the impact).

Given that the probe might not survive, and that liquid impact is possible, and that there will be only one set of data to investigate, development of a software catalogue of impact profiles with some kind of least-squares fitting is probably not justified.

Note that in missions where large sets of data are to be analysed, an automated approach is worthwhile. For example, the accelerometers on the 'snake' guiderope of the Russian Mars 94 balloon used to measure its speed (Powell et al. 1993) of traverse across the ground give a signal that is indicative of the surface that the snake is traversing, and a neural network method has been found to be an effective way of classifying surfaces ('rocky', 'sand', etc.).

Generating some characteristic parameters for the various impact signatures is a useful way of classifying impact types, and of deriving quantitative (albeit uncertain) properties of the surface material.

Two obvious parameters, which are transmitted in the 'quick-look' dataset, are the magnitude fo the peak acceleration signal, and the rise time (the time for the signal to go from 10% to 90% of its peak value) or the time of the peak relative to the start of impact. The materials which correspond to various combinations of these parameters are indicated in figure 7.7.

For the ACC-E signal, for broadly smooth signals, the profile indicates the cohesion of the material. For low-cohesion materials (suchas sand) the force builds up with time: mechanical strength increases with depth. Cohesive materials (clay is the extreme example) jump to an essentially constant value, related to the 'flow pressure' of the material.

Note that, in principle, the ACC-E and accelerometer datasets do not necessarily have to be mutually consistent. The accelerometer signal is sensitive to surface properties averaged over 0.1-1m^2, whereas ACC-E only probes a small fraction of this area. Scenarios can be

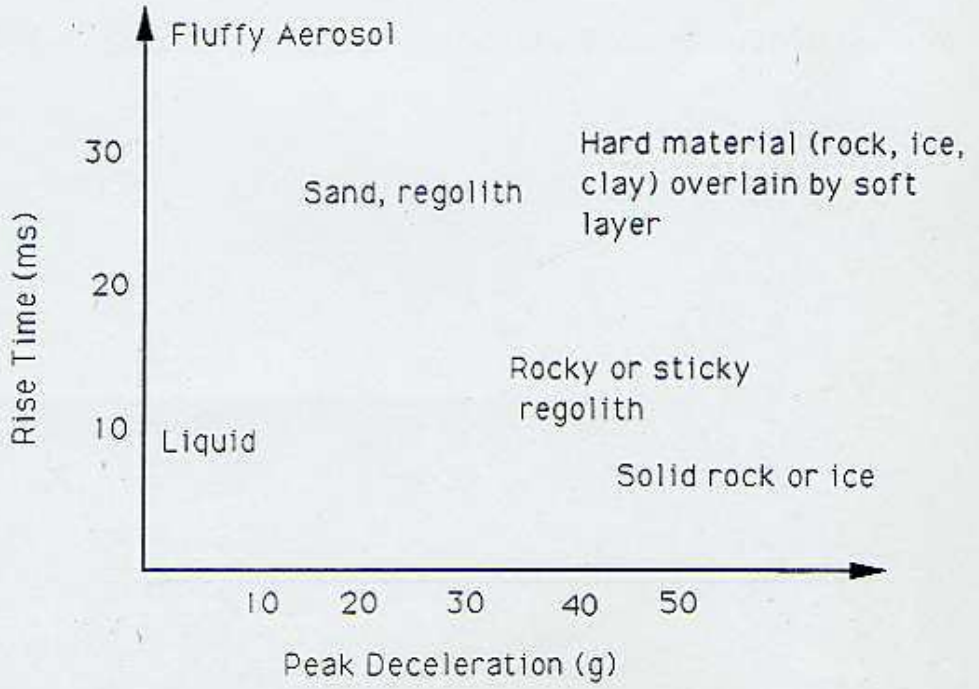

Figure 7.7 Surface material identification map : rise time and peak deceleration allow simple identification of the surface material

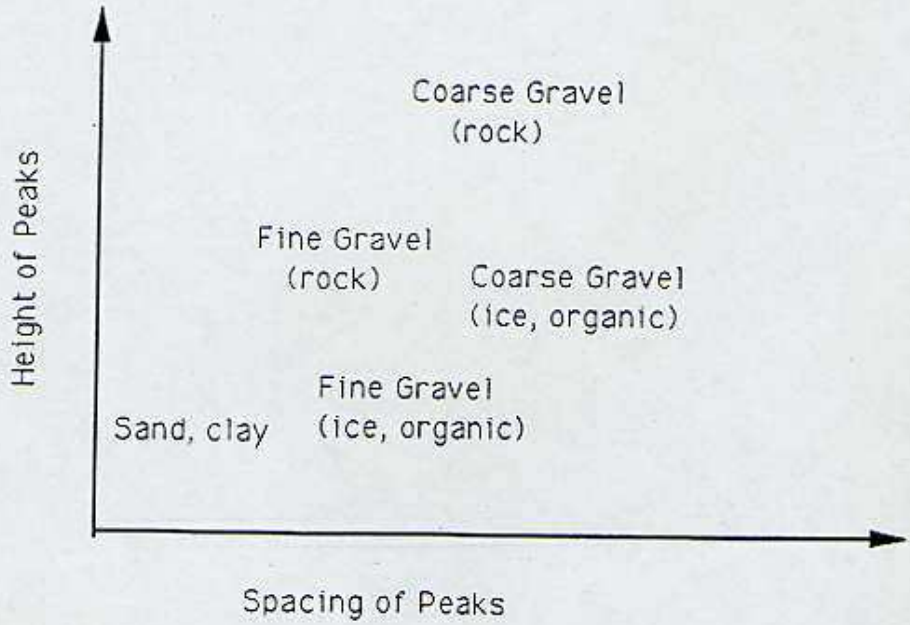

Figure7.8 Particle density determination from penetrometer data: use of peak height and spacing may allow discrimination of low-density materials (e.g. ice) from high density (rock)

envisaged where, for example, ACC-E probes a gravelly gully where fluvial sorting has removed small particles, yet the probe as a whole 'feels' a surface dominated by small cohesive particles.

7.6 Future Work

The work conducted by the author and reported here and in Lorenz 1994b,1994c has shown that the accelerometry and impact penetrometry measurements allow a qualitative identification of the surface materials. Further, if the material is well-sorted in terms of particle size, analysis of the ACC-E profile gives a quantitative indication of particle size, although the measurement suffers from small-sample statistical errors.

As may be seen from the graphs of ACC-E response (figure 7.4) , both the spacing and magnitude of the peaks in the signal correlate with the particle size, Since the magnitude of the peaks presumanly depends on the mass of the particles (rather than their size per se), it may be possible to discriminate btween particles of a given size with low or high density. After estimating the particle size from the peak spacing, the peak magnitudes for this size may be compared with those expected for materials of various densities (see figure 7.8)

Thus, a set of impact profiles for various particle sizes and densities would be valuable: obtaining such a dataset would be a task commensurate with the effort required in a typical undergraduate project. Steel ball-bearings of a variety of sizes are available (ρ=7900 kgm^{-3}); glass spheres (ρ=2900 kgm^{-3}) can be obtained as toy marbles; plastic spheres (ρ~1000 kg m^{-3}) are available also as toys (5mm diameter spheres are used as ammunition in toy guns, for example) and finally, expanded polystyrene spheres (ρ~100 kgm^{-3}) are used in making chemical models. Impact profiles (and the corresponding peak-height and peak-spacing histograms) for these materials, and combinations of them, would be useful.

Additionally, combinations of particle sizes (e.g. a bimodal one of large particles interspersed in a finer medium) and combinations of various particle sizes with binders of varying viscosity (e.g. water, glycerol, clay) would be interesting. Such experiments would be useful not only for Huygens, but also in the context of preparations for measurements on the comet Surface Science Package of the Rosetta mission.

During the experiments reported here (see figure 7.4) the attitude of the penetrometer has been controlled by dropping down a tube. This is quite inconvenient, since the cable must also go down the tube. False triggering due to tube friction occurs, and it is difficult to vary the

impact speed. Additionally, it is not possible to vary the orientation of the penetrometer independent of its velocity (i.e. the penetrometer always points directly along its velocity vector). To allow independent investigation of non-vertical orientation and non-vertical velocity, and apparatus shown in figure 7.9 is suggested for future experiments.

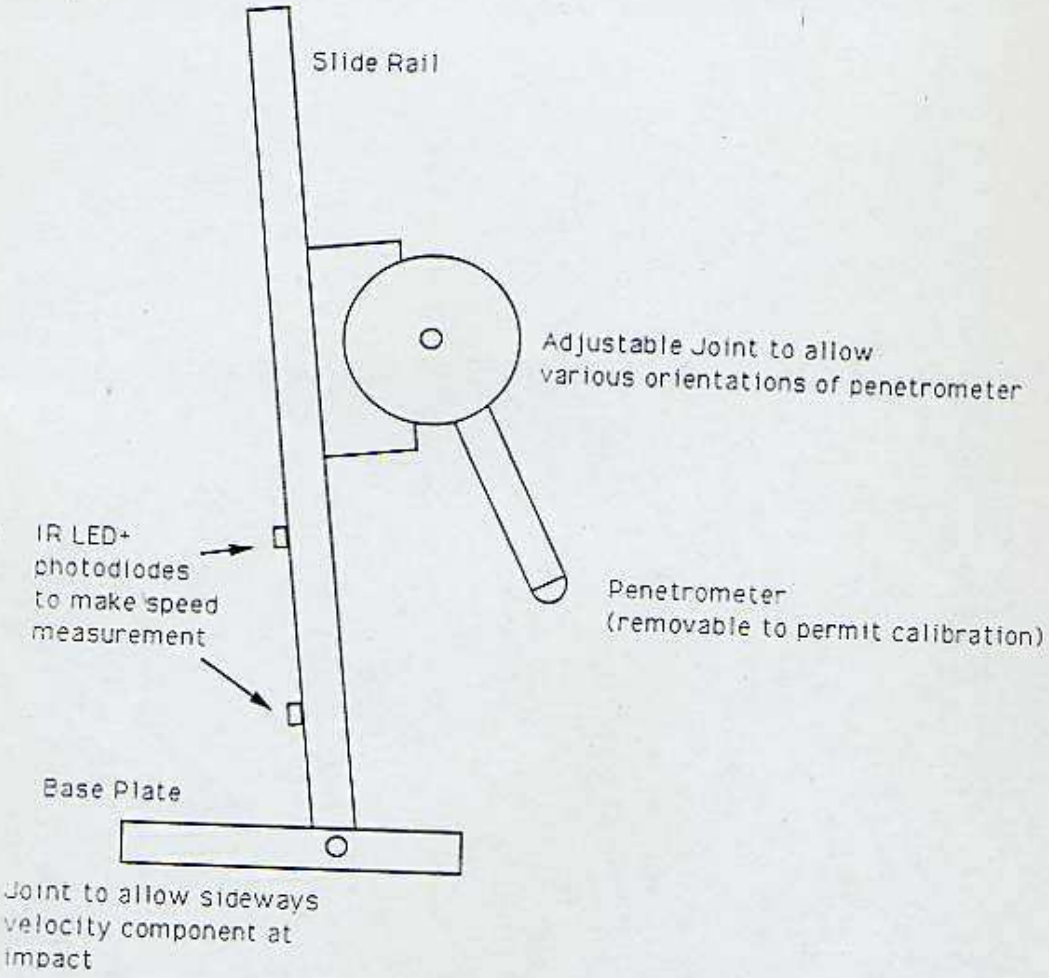

Figure 7.9 Suggested apparatus for future experimentation with penetrometer. Joints allow attitude and direction of motion to be varied. Direct speed measurement allows easy examination of sensitivity to impact velocity. Open rail design allows easy cabling access.

Chapter 8

Acoustic Measurements

The observer listens to nature: the experimented questions and forces her to reveal herself

Georges Cuvier, French Zoologist

Noise proves nothing. Often a hen who has merely laid an egg cackles as if she had laid an asteroid

Mark Twain, American Writer

The potential utility of making acoustic measurements with Huygens was realised early in the study phase, and the project scientist J-P Lebreton encouraged some interest in this area. Ulamec performed some studies (Ulamec 1987, 1990) of the backscatter coefficient of various materials, as well as an investigation of the speed of sound and attenuation coefficient in liquid hydrocarbons.

As mentioned in Chapter 6, the passive acoustic sensing function (with the primary stated aim of searching for lightning) was adopted by HASI, since it already had a DSP function in its electronics. Active acoustic sensing (sounding, and speed of sound measurement) was adopted by SSP in early 1991, with the development being undertaken by L H Svedhem of ESTEC/SSD.

Here I discuss briefly the speed of sound measurement, and then go on to describe the sounder, and how its data may be used to derive information on the surface topography. Some computer simulations and field tests are illustrated. Finally I make some comments on passive acoustic sensing and the acoustic environment on Titan.

8.1 Speed of Sound

In a perfect gas, the speed of sound is given by

$$c=(\gamma R_0 T/M)^{0.5}$$

where γ is the ratio of specific heats (1.4 for nitrogen) R_0 is the universal gas constant (8314 Jkg^{-1} mol^{-1}), T is the absolute temperature and M is the mean molecular weight of the gas. Substituting M=28, T=287 gives c=340 ms^{-1}, the standard value for the speed of sound in air.

In Titan's atmosphere, M~28, T=94K near the surface, so c~200 ms^{-1}. The profile of sound speed as a function of altitude is dominated by the variation in temperature: see figure 8.1. Measurement of the speed of sound poses a constraint on $\gamma T/M$: if temperature is known, then composition (γ/M) can be constrained. Since T should be known with high accuracy by HASI measurements, then measurement of c allows the molecular mass of the atmosphere to be constrained e.g. the range allowed by the V1 RO experiment is 28.3-29.2 at the surface (Samuelson et al., 1981), suggesting nitrogen as the dominant constituent, with the range driven by the mixing ratios of argon (M=40) and methane (M=16). For small mixing ratios of these compounds, the variation in γ (1.4 for nitrogen, 1.313 for methane, 1.667 for argon) is small, and the variation in M controls the sound speed: 20% argon leads to a sound speed ~3% lower than if no argon is present.

Thus a measurement of c gives a useful constraint on atmospheric composition, although it does not determine it uniquely. Further, since the methane abundance in troposphere is controlled by its vapour pressure (and hence is a function of temperature, and altitude) variation in c, where T is known, allows the methane mixing ratio profile to be determined to a useful accuracy, which is important for understanding moist convective processes, for example.

Because a speed of sound measurement is very brief, it can be made frequently - much more frequently than the GCMS can sample atmospheric composition. Thus the vertical resolution of the methane mixing ratio obtained with a speed of sound measurement can be considerably higher than that derived from other instruments such as GCMS (although a PIRLS-type instrument would be considerably better).

The speed of sound measurement on SSP is performed between two transducers mounted at the bottom of the top hat, at the base of the probe. The transducers are separated by ~14cm, leading to a 1 way trip time of ~0.7ms.

The altitude at which these measurements can start is driven by the efficiency of coupling between the transducers (bimorph piezoelectric elements) and the atmosphere, this coupling being driven by the ratio of acoustic impedances (acoustic impedance = density*speed of sound). Thus at high altitude (low atmospheric density) the impedance is very low (see figure 8.2), and the coupling is inefficient, so the signal-to-noise ratio for reception of the signal becomes too low. (This problem is in part exacerbated by the fact that the transducer design is a compromise

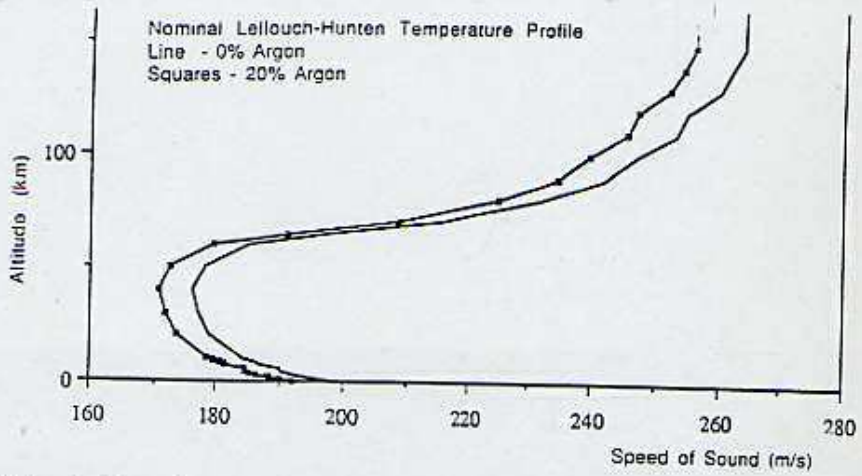

Figure 8.1 Speed of Sound in Titan's Atmosphere, with and without Argon

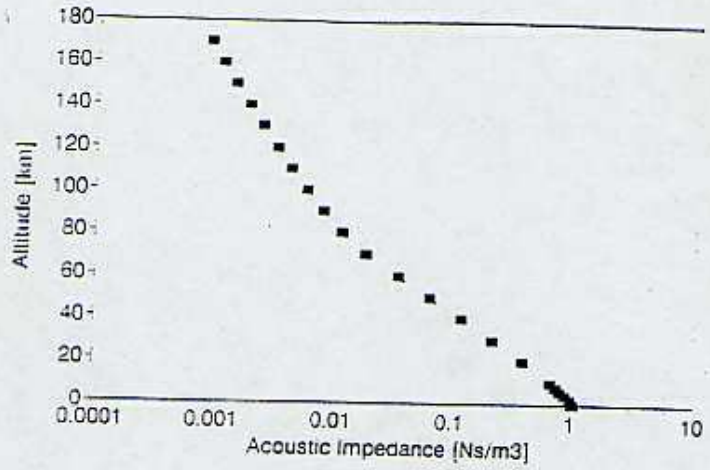

Figure 8.2 Acoustic Impedance of Titan's Atmosphere

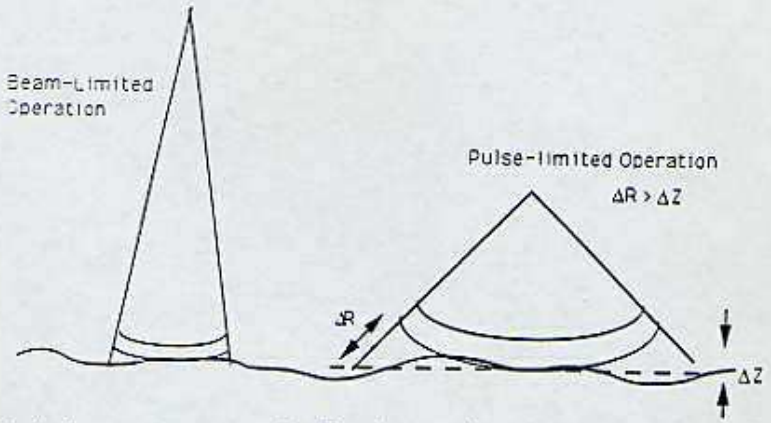

Figure 8.3 In beam-limited operation, a sounder illuminates only a tiny patch of the surface. When the beam is wide enough that the slant range ΔR exceeds the surface roughness scale ΔZ, the sounder is termed 'pulse-limited'.

between atmospheric performance and performance in an ocean). Currently it is anticipated that speed of sound measurements will be able to take place from an altitude of ~100km.

The altitude resolution is dictated by data rate constraints, which limit the frequency with which the measurements can be made. Measurements are recorded once per second, leading to an altitude resolution profile that mirrors the descent velocity (see Figure 5.8), reaching about 5m near the surface.

The time of flight of the signal is measured with an accurate clock . Assuming the transducer-transducer distance is known to 0.5mm (recall that the transducers distort in order to function, and there may be some slight deformations of the probe and SSP structure due to aerodynamic loads and temperature effects) then the speed of propagation of the sound pulse will be known with an accuracy of ~0.3%. An additional problem (Svedhem, private communication) is that to keep the pulse bandwidth sufficiently narrow, the pulse itself must be quite wide. Thus an accuracy of ~0.5% may be expected.

The speed of propagation in one direction could be influenced by the component of any wind velocity in the propagation direction (indeed acoustic anemometers are quite widely used in meteorological applications, and especially in measuring turbulence for pollution or gas transport studies, due to the high rate of measurement). However, the measurement is made in both directions to counter this potential problem, and the transducers are recessed slightly from the front of the probe in any case, minimising the influence of wind on the measurement.

In an ocean, the speed of sound measurement is a useful diagnostic of composition. Ulamec (1987) evaluated the speed of sound for various ethane/methane mixtures, varying between 1535 ms^{-1} for methane and 1977 ms^{-1} for ethane, although he did not investigate the effects of argon, nitrogen and other solutes. Taking these factors into account, and assuming the speed of sound can be measured to an accuracy of 0.5%, then the ethane mole fraction can be determined with an accuracy of the order of ~ 5% (see chapter 6).

In addition to providing a constraint on ocean composition, the speed of sound measurement is of direct relevance to the interpretation of data from the sounder, both in the atmosphere, and more importantly in the ocean, where the sounder will constrain the depth.

8.2 Sounder

The original rationale for the sounder was as a means of establishing a lower limit on ocean depth. However, it was realised that sounding measurements of the surface could be performed shortly before impact, to evaluate surface topography.

The principle of the sounding measurement is simple: a pulse of sound is transmitted, and the reflected signal received, and its time-of-flight noted. At its most simple level, if the beam from the transducer is considered to be small, the measurement gives the range between the transducer and the 'illuminated' spot on the surface: an altimetric profile could be built by allowing the spot to traverse the surface due to the horizontal displacement of the probe by winds. The spot could also be 'painted' around by pendulum motion of the parachute.

However, such 'beam-limited' operation has disadvantages: first, the spot only samples a small region of the surface. Second, while a narrow beam gives good range performance due to the high transmit and receive gain, this requires good attitude control of the probe (to a first order, the attitude of the probe should not change by an angle of the order of the half-beamwidth of the transducer during the propagation time of the signal. The attitude specification for the descent control system on Huygens is 0.6°/s, imposed by DISR to prevent motion blur, and would correspond to a half-beamwidth of about 1° for a measurement from 200m altitude.

On Huygens the beamwidth question is largely academic, since antenna theory shows that to generate a beamwidth of θ requires a transducer diameter D of the order of θ/λ. In the low sound speed environment on Titan, with c~200 ms^{-1}, and for realistic frequencies ~10kHz (see later) λ~2cm. For straightforward accommodation on SSP, D is limited to ~10cm, so the beamwidth is at least ~0.2 radians, or ~10°. With such a large beamwidth, the sounder is no longer 'beam-limited', but 'pulse-limited'. For a discussion of these two modes in the context of radar altimeters, see Rapley (1990) : see also figure 8.3.

In pulse-limited operation, the footprint (spot) of the transducer is relatively large. However, because the range to the centre of the spot is considerably less than that to the edge of the spot, and the propagation times are correspondingly different, the echo of the transmitted pulse is smeared out. The altimetric accuracy of a beam-limited device is clearly better, since the echo pulse is unsmeared, but the shape of a beam-limited device contains information on the topography within the footprint. For a detailed description of the smearing process, see Brown (1977), and the following section.

The choice of operating frequency for the sounder is driven by a compromise between strong attenuation of high-frequency sound (and the thermal generation of noise at these frequencies) in the atmosphere, and the likely aeroacoustic noise generated by the flow around the probe (see figure 8.4) . The optimum operating frequency was felt initially to be around 35kHz (Svedhem 1990), but a subsequent study (Broch 1991) suggested 20kHz. Transducer performance is also a factor, so the implemented frequency is in the range 15-20kHz.

8.3 Computer Simulations of Sounder Operation

In order to investigate what can be learned from the shape of the echo signal from Titan's surface, and to define the useful sampling rates and digitisation accuracy for the sounder, computer simulations were performed.

The acoustic sounder function on Huygens carries an important complication, not found with classical radar altimeters: the platform (probe) velocity is a significant fraction of the propagation speed of the signal, such that the transmission point of the sound pulse, and its reception point cannot be considered to be co-located. E.g. for a 200m altitude, the sound pulse takes 2s to return, during which time the probe has descended 10m. Since this distance is appreciable compared with the footprint size and the expected topographic variation, a correction must be applied. Where the transmitter and receiver of a radar or sonar system are colocated, the isochrones (or contours of equal propagation time) are spherical: where the two are displaced by some distance, the isochrones become ellipsoidal.

For these initial simulations, the probe is assumed to be descending vertically with aspeed v. The transmit pulse is d wide, and is transmitted and received by a transducer whose gain G for an angle ϕ is described by

$$\left.\begin{array}{l} G = G_0 \cos(\pi\phi/2\theta) \text{ for } \phi<1.5\theta \\ G=0 \text{ for } \phi>1.5\theta \end{array}\right\} \quad (1)$$

with G_0 the boresight gain, and 2θ is the FWHM beamwidth mentioned earlier

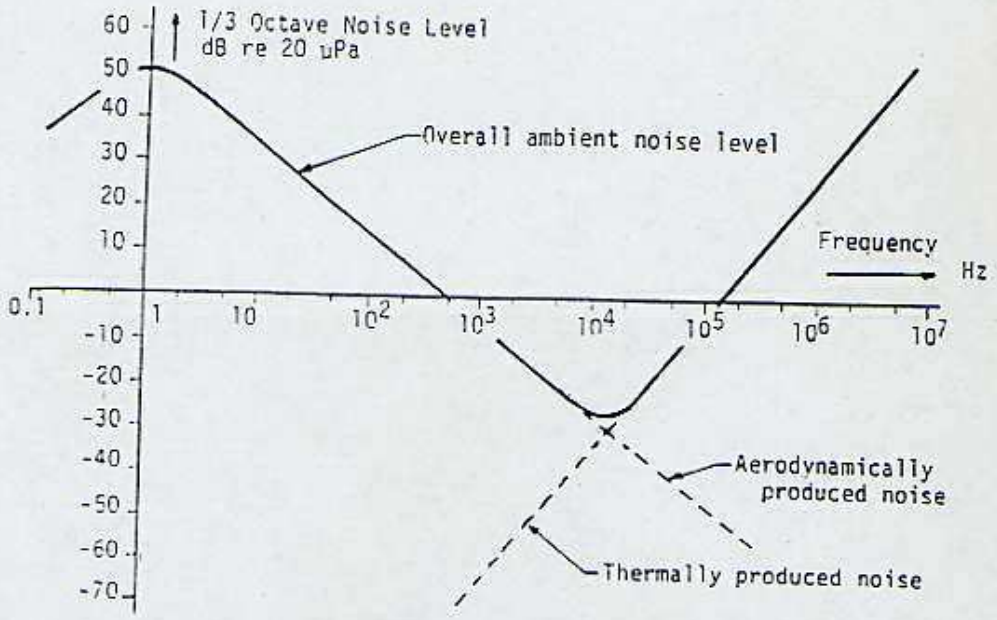

Figure 8.4 Acoustic environment during probe descent. API-S operation occurs near the noise minimum at about 20kHz (Figure taken from Broch 1991)

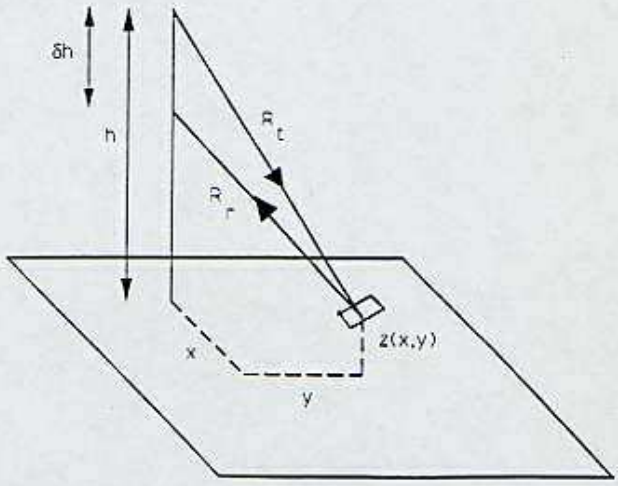

Figure 8.5 Geometry for echo simulations : signal from probe at altitude h bounces from surface element at height z(x,y) and returns to probe, which has descended by a height δh during the transit time

The boresight is assumed to be vertical. The probe is assumed to be a height h above the nominal surface. The surface topography is described by a function z=f(x,y) where x and y are orthogonal coordinates in the horizontal plane, with the sub-probe point at the origin: see figure 8.5.

Thus the transmit range to a point is

$$R_t = ((h-z(x,y))^2 + x^2 + y^2)^{0.5} \qquad (2)$$

and the one-way propagation time =R/c. To a first order, during the two-way trip of the sound pulse, the probe will have descended a distance δh, where

$$\delta h \sim 2vR_t/c \qquad (3)$$

and the corresponding receive range is

$$R_r = ((h-\delta h-z(x,y))^2 + x^2 + y^2)^{0.5} \qquad (4)$$

Thus the two-way trip time is

$$t = (R_t + R_r)/c \qquad (5)$$

(strictly speaking, since $R_r < R_t$, $\delta h < 2vR_t/c$ these expressions slightly underestimate t, but the error is of order $(v/c)^2$, and can therefore be ignored).

The magnitude of the echo component from this point z(x,y) is computed as follows. The transmit pulse has an energy P. The transmit angle ϕ_t is given by

$$\tan \phi_t = ((x^2+y^2)^{0.5}/(h-z(x,y))) \qquad (6)$$

and the transmit gain G_t computed from equation X above. The signal is attenuated by a free space loss (atmospheric attenuation is ignored) of $1/R_t^2$, and intercepted by the scattering area dA at (z,x,y). It is assumed the surface has a unity reflection coefficient, and scatters isotropically, so the return echo is attenuated by a factor $1/2\pi R_r^2$, and multiplied by a gain G_r, determined from equ.1 above using

$$\tan \phi r = ((x2+y2)0.5/(h-dh-z(x,y))) \quad (7)$$

Thus the echo strength S is

$$S=PG_tG_rdA/R_t^2R_r^2 \quad (8)$$

The echo shape is formed as follows: a set of echo time bins E(t) are set up (e.g. 1ms wide) and a computer program steps through an array of surface positions (x,y) calculating the echo times and strengths as above. For each (x,y) position, the corresponding time bin has its value incremented by the echo strength S(x,y). The resultant profile is then smoothed by convolving with a square window dt wide, to take account of the finite width of the transmit pulse.

Note that I have not been rigorous in preserving conventions of definitions of gain, backscatter coefficient etc., and units are arbitrary: the object of the exercise was to see how the *shape* of the echo pulse was influenced by the topography, and thereby to define sampling rate and resolution requirements for the flight instrument.

For the simulations, performed in Autumn 1991, a 30x30 grid of (x,y) points was assumed, with $dA=1m^2$. These values correspond approximately to the footprint defined by the probe 100m above the surface. Processor speed and memory limitations prevented higher-fidelity simulations being performed (in principle, it would be useful to have an (x,y) grid with spacing equivalent to the altitude resolution of the sensor, namely ~10cm.). However, these simulations showed that useful topographic information could be recovered if the echo was sampled at ~1kHz, with the relative magnitude of the signal (it was assumed the sensor would have some kind of automatic gain control (AGC) to limit the dynamic range needed) measured to ~6 bits : these allowed practicable data rate and volume allocations to be defined for the API-S

Some sample surfaces and their echoes are shown in figures 8.6 and 8.7.

The response from the flat, horizontal surface (figure 8.6a) is quite short (like the transmit pulse), but slightly rounded and smeared due to the combined effect of beam shape and range spread within the footprint. As the slope of the surface is increased (figures 8.6b-8.6d) the decay part of the echo pulse becomes shallower. Correlation of the probe attitude, measured with TIL, and the decay slope, should be able therefore to indicate the surface slope.

The original rationale for the sounder was as a means of establishing a lower limit on ocean depth. However, it was realised that sounding measurements of the surface could be performed shortly before impact, to evaluate surface topography.

The principle of the sounding measurement is simple: a pulse of sound is transmitted, and the reflected signal received, and its time-of-flight noted. At its most simple level, if the beam from the transducer is considered to be small, the measurement gives the range between the transducer and the 'illuminated' spot on the surface: an altimetric profile could be built by allowing the spot to traverse the surface due to the horizontal displacement of the probe by winds. The spot could also be 'painted' around by pendulum motion of the parachute.

However, such 'beam-limited' operation has disadvantages: first, the spot only samples a small region of the surface. Second, while a narrow beam gives good range performance due to the high transmit and receive gain, this requires good attitude control of the probe (to a first order, the attitude of the probe should not change by an angle of the order of the half-beamwidth of the transducer during the propagation time of the signal. The attitude specification for the descent control system on Huygens is 0.6°/s, imposed by DISR to prevent motion blur, and would correspond to a half-beamwidth of about 1° for a measurement from 200m altitude.

On Huygens the beamwidth question is largely academic, since antenna theory shows that to generate a beamwidth of θ requires a transducer diameter D of the order of θ/λ. In the low sound speed environment on Titan, with c~200 ms^{-1}, and for realistic frequencies ~10kHz (see later) λ~2cm. For straightforward accommodation on SSP, D is limited to ~10cm, so the beamwidth is at least ~0.2 radians, or ~10°. With such a large beamwidth, the sounder is no longer 'beam-limited', but 'pulse-limited'. For a discussion of these two modes in the context of radar altimeters, see Rapley (1990) : see also figure 8.3.

In pulse-limited operation, the footprint (spot) of the transducer is relatively large. However, because the range to the centre of the spot is considerably less than that to the edge of the spot, and the propagation times are correspondingly different, the echo of the transmitted pulse is smeared out. The altimetric accuracy of a beam-limited device is clearly better, since the echo pulse is unsmeared, but the shape of a beam-limited device contains information on the topography within the footprint. For a detailed description of the smearing process, see Brown (1977), and the following section.

The choice of operating frequency for the sounder is driven by a compromise between strong attenuation of high-frequency sound (and the thermal generation of noise at these frequencies) in the atmosphere, and the likely aeroacoustic noise generated by the flow around the probe (see figure 8.4) . The optimum operating frequency was felt initially to be around 35kHz (Svedhem 1990), but a subsequent study (Broch 1991) suggested 20kHz. Transducer performance is also a factor, so the implemented frequency is in the range 15-20kHz.

8.3 Computer Simulations of Sounder Operation

In order to investigate what can be learned from the shape of the echo signal from Titan's surface, and to define the useful sampling rates and digitisation accuracy for the sounder, computer simulations were performed.

The acoustic sounder function on Huygens carries an important complication, not found with classical radar altimeters: the platform (probe) velocity is a significant fraction of the propagation speed of the signal, such that the transmission point of the sound pulse, and its reception point cannot be considered to be co-located. E.g. for a 200m altitude, the sound pulse takes 2s to return, during which time the probe has descended 10m. Since this distance is appreciable compared with the footprint size and the expected topographic variation, a correction must be applied. Where the transmitter and receiver of a radar or sonar system are colocated, the isochrones (or contours of equal propagation time) are spherical: where the two are displaced by some distance, the isochrones become ellipsoidal.

For these initial simulations, the probe is assumed to be descending vertically with aspeed v. The transmit pulse is d wide, and is transmitted and received by a transducer whose gain G for an angle ϕ is described by

$$\left.\begin{array}{l} G = G_0 \cos(\pi\phi/2\theta) \text{ for } \phi<1.5\theta \\ G=0 \text{ for } \phi>1.5\theta \end{array}\right\} \quad (1)$$

with G_0 the boresight gain, and 2θ is the FWHM beamwidth mentioned earlier

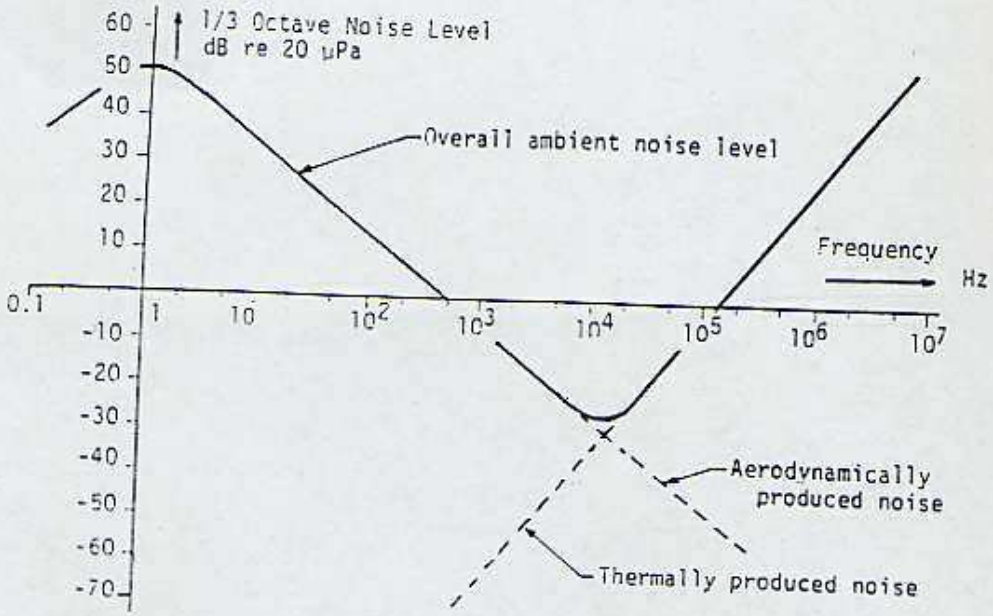

Figure 8.4 Acoustic environment during probe descent. API-S operation occurs near the noise minimum at about 20kHz (Figure taken from Broch 1991)

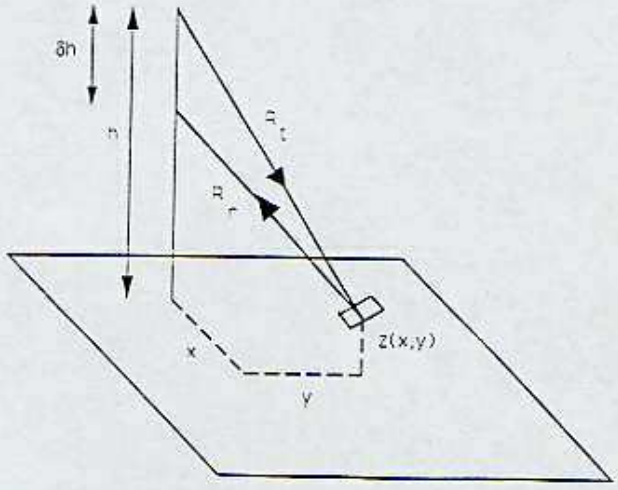

Figure 8.5 Geometry for echo simulations : signal from probe at altitude h bounces from surface element at height z(x,y) and returns to probe, which has descended by a height δh during the transit time

The boresight is assumed to be vertical. The probe is assumed to be a height h above the nominal surface. The surface topography is described by a function z=f(x,y) where x and y are orthogonal coordinates in the horizontal plane, with the sub-probe point at the origin: see figure 8.5.

Thus the transmit range to a point is

$$R_t = ((h-z(x,y))^2 + x^2 + y^2)^{0.5} \qquad (2)$$

and the one-way propagation time =R/c. To a first order, during the two-way trip of the sound pulse, the probe will have descended a distance δh, where

$$\delta h \sim 2vR_t/c \qquad (3)$$

and the corresponding receive range is

$$R_r = ((h-\delta h-z(x,y))^2+x^2+y^2)^{0.5} \qquad (4)$$

Thus the two-way trip time is

$$t = (R_t+R_r)/c \qquad (5)$$

(strictly speaking, since $R_r<R_t$, $\delta h<2vR_t/c$ these expressions slightly underestimate t, but the error is of order $(v/c)^2$, and can therefore be ignored).

The magnitude of the echo component from this point z(x,y) is computed as follows. The transmit pulse has an energy P. The transmit angle ϕ_t is given by

$$\tan \phi_t = ((x^2+y^2)^{0.5}/(h-z(x,y))) \qquad (6)$$

and the transmit gain G_t computed from equation X above. The signal is attenuated by a free space loss (atmospheric attenuation is ignored) of $1/R_t^2$, and intercepted by the scattering area dA at (z,x,y). It is assumed the surface has a unity reflection coefficient, and scatters isotropically, so the return echo is attenuated by a factor $1/2\pi R_r^2$, and multiplied by a gain G_r, determined from equ.1 above using

$\tan \phi r = ((x2+y2)0.5/(h-dh-z(x,y)))$ (7)

Thus the echo strength S is

$S=PG_tG_rdA/R_t^2R_r^2$ (8)

The echo shape is formed as follows: a set of echo time bins E(t) are set up (e.g. 1ms wide) and a computer program steps through an array of surface positions (x,y) calculating the echo times and strengths as above. For each (x,y) position, the corresponding time bin has its value incremented by the echo strength S(x,y). The resultant profile is then smoothed by convolving with a square window dt wide, to take account of the finite width of the transmit pulse.

Note that I have not been rigorous in preserving conventions of definitions of gain, backscatter coefficient etc., and units are arbitrary: the object of the exercise was to see how the *shape* of the echo pulse was influenced by the topography, and thereby to define sampling rate and resolution requirements for the flight instrument.

For the simulations, performed in Autumn 1991, a 30x30 grid of (x,y) points was assumed, with $dA=1m^2$. These values correspond approximately to the footprint defined by the probe 100m above the surface. Processor speed and memory limitations prevented higher-fidelity simulations being performed (in principle, it would be useful to have an (x,y) grid with spacing equivalent to the altitude resolution of the sensor, namely ~10cm.). However, these simulations showed that useful topographic information could be recovered if the echo was sampled at ~1kHz, with the relative magnitude of the signal (it was assumed the sensor would have some kind of automatic gain control (AGC) to limit the dynamic range needed) measured to ~6 bits : these allowed practicable data rate and volume allocations to be defined for the API-S

Some sample surfaces and their echoes are shown in figures 8.6 and 8.7.

The response from the flat, horizontal surface (figure 8.6a) is quite short (like the transmit pulse), but slightly rounded and smeared due to the combined effect of beam shape and range spread within the footprint. As the slope of the surface is increased (figures 8.6b-8.6d) the decay part of the echo pulse becomes shallower. Correlation of the probe attitude, measured with TIL, and the decay slope, should be able therefore to indicate the surface slope.

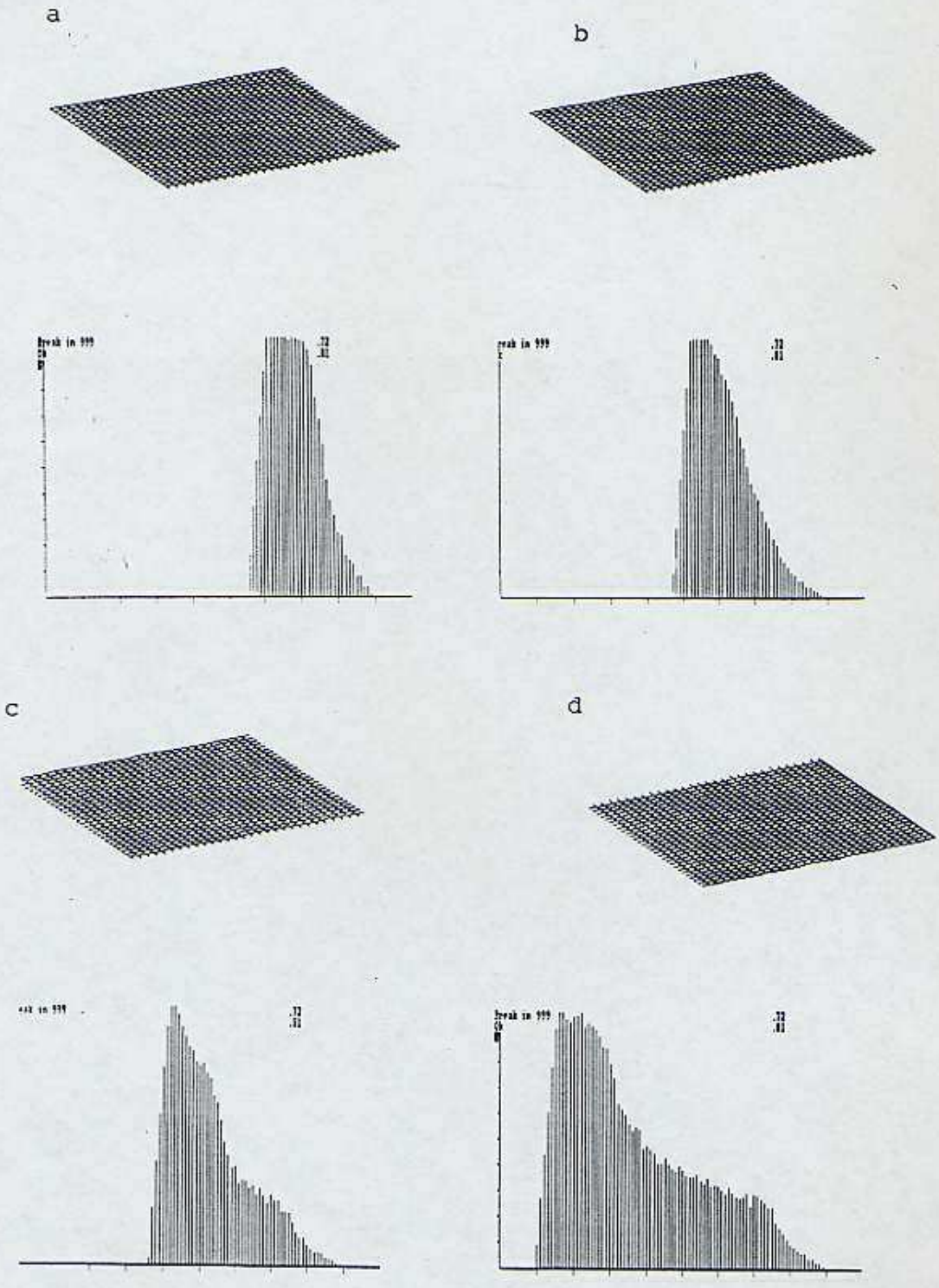

Figure 8.6 Simulated echo shapes from various flat surfaces. Each panel shows the simulated surface, and the amplitude profile of the returned echo. The surface is 30m square: echo amplitude is in arbitrary units. Echoes are for h=100m; the abscissa (echo time) runs from 0.72 to 0.81 seconds on each graph. Surfaces are flat, with slopes 0 (a), 1 in 20 (b), 1 in 10 (c) and 1 in 5 (d)

The response from a faulted surface (figure 8.7a), with two flat, horizontal sections vertically displaced from each other by 2m, gives an echo that essentially comprises 2 almost discrete components, each similar to the flat surface response.

A wavy (sinusoidal) surface, which could be caused by ocean swell, or perhaps sand dunes, has a characteristic double-peaked 'saddle' echo (figure 8.7b), although note that in principle other topographies could also generate such an echo. In some laboratory experiments conducted in a small wave tank, Ulamec and Svedhem (1992) noted that wavy surfaces gave a double-peaked echo shape.

Two rough surfaces (in 8.7c, generated by adding some gentle 'bumps' to a flat surface, and in 8.7d by repeatedly faulting a flat surface) have broad, irregular echoes, with shallow attack and decay slopes.

These simulations show clearly how topography may be inferred to a first order from a single echo shape. The simulations suffer some limitations, however. Small changes in parameters (e.g. the probe height) lead to noticeable changes in the echo profile, suggesting that 'quantization noise' due to the relatively coarse topography grid is present. Further, it is assumed that all surfaces are illuminated by the transmit signal: in principle if the topography is steep, some surface areas could be shadowed. Further, the isotropic scattering assumed is not valid for all surfaces: flat surfaces could lead to significant specular reflections. Also, the effect of varying reflection coefficient as well as surface height over the footprint has not been studied.

The author began considering how successive echoes could be combined to build up a topographic map: since each echo in principle contains information on the distribution of surface height z for a ring of constant (x^2+y^2). Wind drift, pendulum motion, and the shrinking footprint of the transducer would allow some topography reconstruction.

One method would be to define a surface height probability space p(x,y,z). Knowing the probe trajectory (and it is not yet clear exactly how well this can be reconstructed) then for each transmit location and for each echo time bin, an isochronic ellipse can be defined. The probability of a scatterer (e.g the surface) being present at a location (x,y,z) is presumably higher if (x,y,z) is on one of these isochrones. Thus each element p(x,y,z) on each isochrone for each transmit pulse should be incremented by a quantity related to the strength of the echo, range, uncertainty on probe attitude and position, etc. A topographic map could be derived by setting z(x,y) equal to the

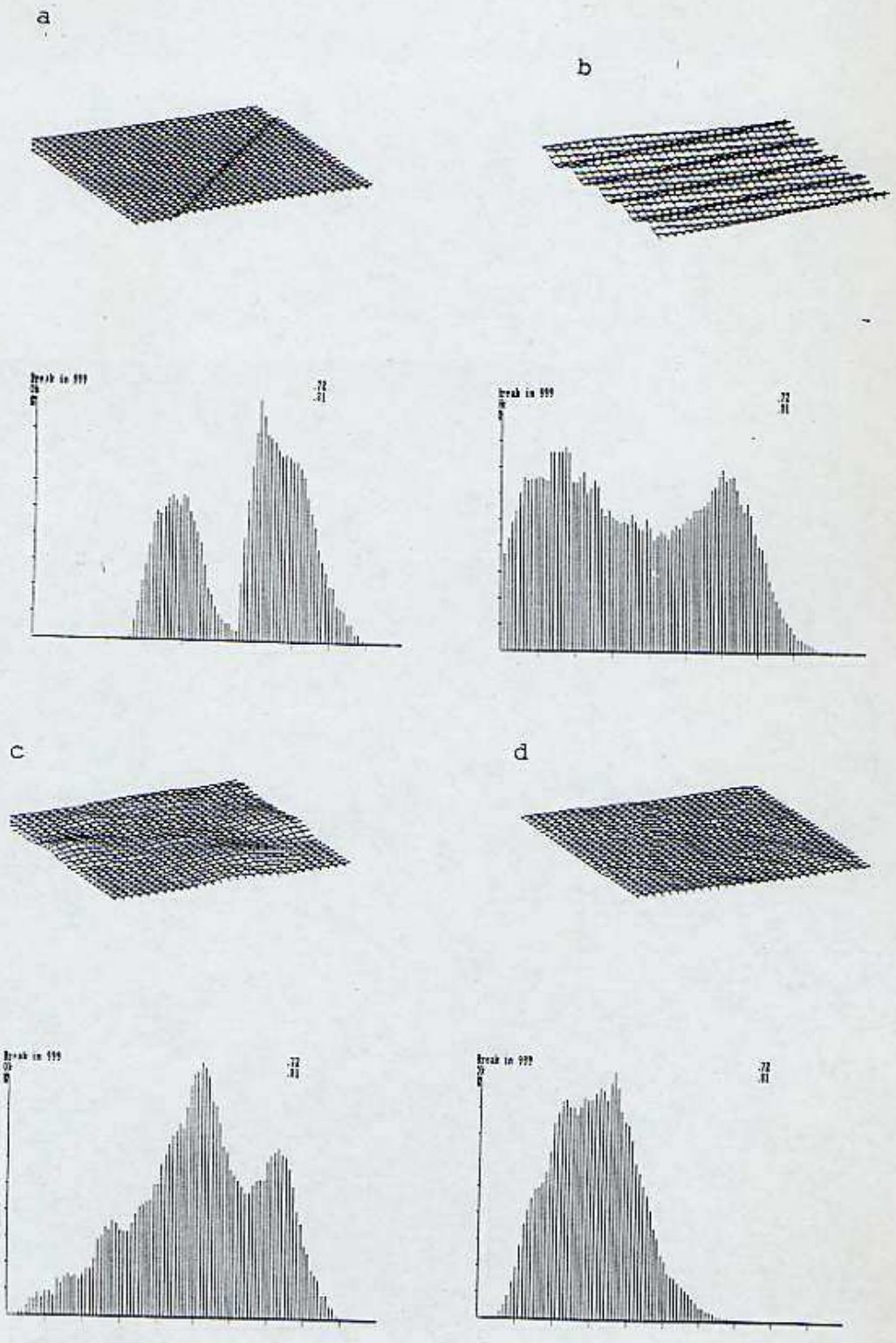

Figure 8.7 Simulated echo shapes from various 'textured' surfaces. Conditions and graph axes as in figure 8.6. Panel a shows a surface with a 3m fault. Panel b shows a sinusoidal surface wavelength ~7m, peak-to-trough height 6m . Panel c shows a surface with bumps, maximum height 6m. Panel d shows a 'cliffy' surface, formed by multiple faulting, again maximum height 6m.

value of z_i for which $p(x,y,z_i)$ was a maximum, after all the increments for all available echoes had been applied. The method is attractive because it would also offer a measure of how uncertain the topographic profile is, although would be computationally intensive.

While beyond the scope of the present thesis, an investigation of this topography reconstruction process would be an interesting and valuable exercise (especially for someone with a talent for computing), and would be directly applicable to API-S data reduction, and that for the radar altimeter.

8.4 Field Test

In order to supplement the simulations described above, outdoor experiments were planned for a prototype sounder. Small-scale tests are readily possible, but it is not clear how representative these would be of real outdoor surfaces, especially when model surfaces have variations over scales of the order of one wavelength and near-field effects become significant. A natural problem with outdoor tests is how to achieve clutter-free separation from target surfaces (e.g. buildings, cliffs) without getting scatter and multipath effects from the ground. The obvious solution is to perform the measurements from an aerial platform of some sort.

Fixed-wing aircraft are generally too fast and noisy to make this practicable. Even hang-gliders have significant wind-speed and aeroacoustic noise, plus operation of a sodar would be distracting. Helicopters would be an ideal platform , but are also very noisy, and expense is an important consideration. Suspension from a crane might be practicable if one were found near a target site of interest, but convenience and expense are factors. (Interestingly, ultrasonic altimeters have been considered for VSTOL aircraft, despite their noise - Maeda et al., 1970)

A lighter-than-air platform would be ideal, since it can be placed over any target of interest (weather permitting) and does not require continuous propulsion. The author visited the Vosper Thorneycroft hangar on Southampton water in February 1992 and flew in the D2 human-powered dirigible (165m^3 helium capacity) designed and built by Dr Graham Dorrington and his students of the Department of Aeronautics and Astronautics, University of Southampton (Dorrington, 1994).

There were considerable delays in the manufacture and procurement of suitable portable sonar and data logging equipment, and the Southampton airship programme was interrupted by a fatal

accident in Sumatra in March 1993. Thus the planned campaign of airborne measurements never took place.

In summer 1994, portable sonar equipment was finally ready, but using large-beamwidth transducers (tweeters for stereo music speakers). The operating frequency was set at 10kHz, to be comparable with the API-S performance, but with lower atmospheric attenuation, and to be easily audible to verify correct experiment operation. The 10kHz signal was sent as a 5ms burst. As with radar equipment, the receiver (even though it used a separate transducer) had to be suppressed by a transmit gate, to prevent saturation as the transmit pulse was sent. The received echo is amplified and sampled by an ADC mated with a portable PC. The whole equipment is battery powered.

The low directionality implies low gain, so only large targets could be 'pinged', and only at ranges of a few metres. Indoor experiments proved to be unsatisfactory, due to multiple echoes. Outdoor experiments were performed under cover of darkness, to ensure low ambient noise, and to minimise embarrassment to the experimenter.

Results are shown in figure 8.8 . Although reproducability was sometimes poor, especially due to false triggering (cf figures 8.8a and b) and the shapes almost defy interpretation, qualitative discrimination between targets is at least possible. No attempt has been made to model these echoes with the simulation method above, in part due to the poorly-controlled conditions (pointing of the transducers and their beamshape) and the variability of the shape of the transmit pulse (often saddle-shaped, rather than square).

Figures 8.8a and b show echoes from the front of the UKC physics building, which is flat The echo is quite spread, in part due to the large beamwidth of the transducers. Note, however, the steep attack of the echo shape. The slow decay or after-echo may be in part due to multipath involving ground reflection.

Figure 8.8c shows an echo from a bushy tree. The 'scattering volume' nature of this target, and its rounded shape, give a much shallower attack slope.

Figure 8.8d shows a barely-detectable echo from the side of the UKC library. This building has a 'boxy' buttressed wall, resembling a mortice, or castellation. There are essentially two reflection

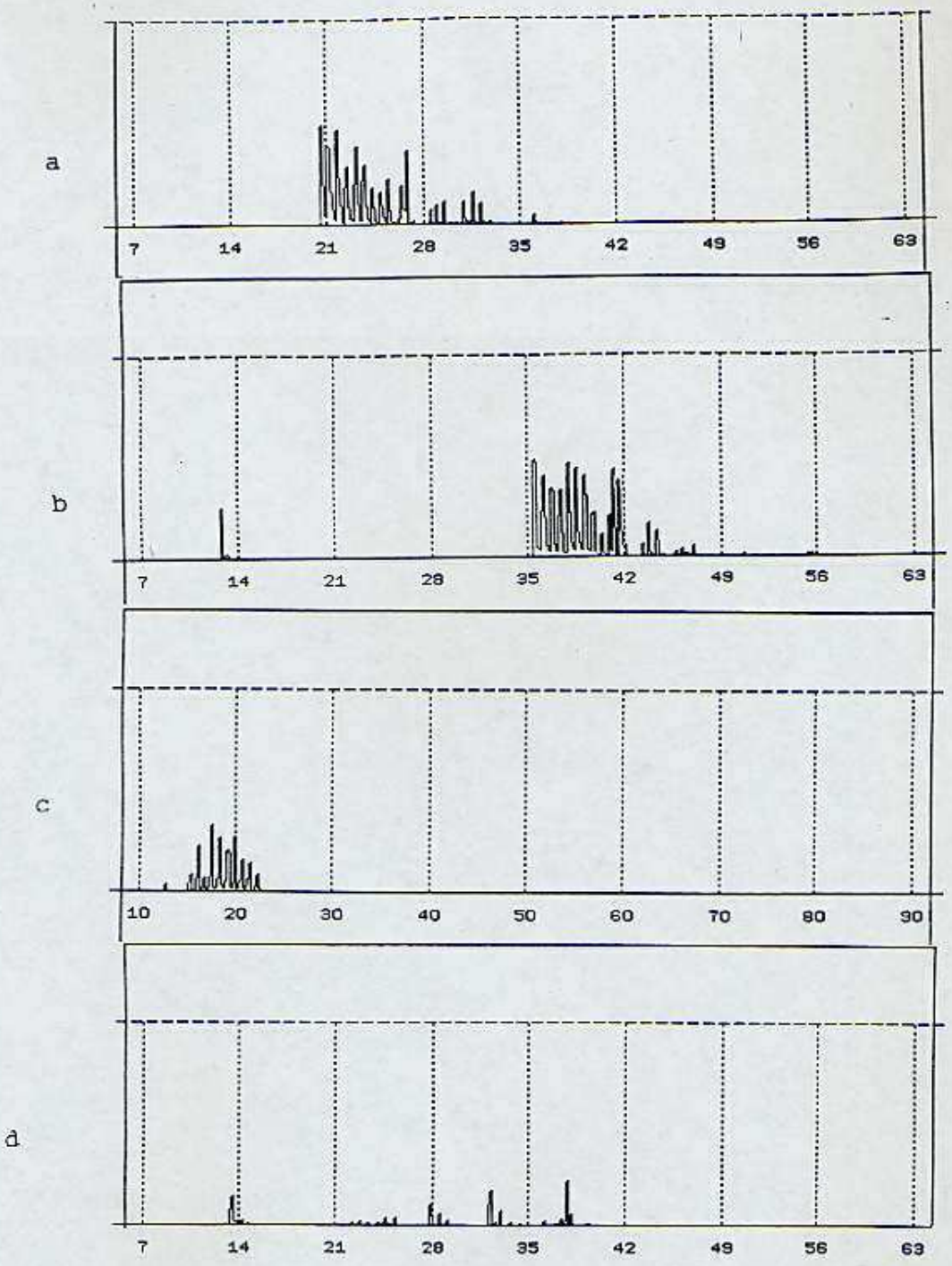

Figure 8.8 Field test echo measurements; abscissa is time in milliseconds. Panels a and b show echoes from the flat wall of the UKC physics building at ~4m (note in panel b that the timing of the return pulse looks incorrect, as the sampling system has been spuriously triggered. The small spike at ~12ms is the tail end of the transmit pulse which has not been suppresed by the receiver gate. The difference between this spike and the start of the echo at 35ms is ~21ms, the same as in panel a) Panel c shows echo from a bushy tree at ~2m. Panel d shows the echo from the UKC library building's 'castellated' wall.

targets, spaced in range by about 1.5m, leading to the multiple echo (consider two attenuated echoes like 8.8a, spaced by ~10ms, and the result superficially resembled figure 8.8d).

Thus, the field measurements broadly show that, as indicated by the simulations, useful topographic information can be inferred from echo shape. However, the field tests to date are somewhat unsatisfactory. Future experiments, using more powerful (and more importantly, more directional) transducers, would be of great benefit. Further, airborne measurements would aid interpretation by eliminating multipath effects.

8.5 Passive Acoustic Sensing

The SSP API-S subsystem is able in principle to record background or ambient noise within its passband (currently 20kHz+/-500Hz, the bandwidth dictated by doppler shift expected by the probe's motion near the surface, with an appropriate margin)

Additionally, the HASI PWA system includes a wideband microphone, able to record (by using the DSP chip of PWA) the power spectrum of ambient noise from a few Hz to 5kHz, with a resolution of the order of 50Hz.

What might these instruments record? Clearly during descent (see figure 8.4) there will be a substantial aeroacoustic component. On the ground, however, this noise will cease. Probe-generated noise on the surface is likely to be small - the ACP pump will have been shut down, so the only piece of moving equipment on the probe is the tiny shutter on the DISR infrared channels, which is unlikely to produce a large acoustic signal.

Ksanfomality et al. (1983b) were able to infer near-surface windspeeds on Venus by comparing the amplitude of noise recorded by a microphone on the Venera 12 and 13 landers with that obtained by microphones on models in a wind tunnel. A similar surface windspeed measurement might be possible on Huygens, and would be extremely valuable, especially if a landing-induced dustcloud was present.

Other noise sources such as rain, distant volcanoes, thunder etc. can be speculated upon, but one noise source is worth investigating, namely that of undersea bubbles. Rainfall and wave action can lead to the entrainment of bubbles of atmosphere, which eventually float upwards and burst at

the surface, often yielding small aerosol particles. These bubbles play an important role in transporting materials across the ocean-atmosphere interface.

Bubbles oscillate like little bells, and it is this oscillation that leads to the pleasant musical 'tinkling' sound of water familiar to us on Earth. The frequency of the oscillation f of a bubble was investigated by Minnaert (1927), who gave the following expression

$$f = (1/\pi d)(3\kappa P_o/\rho)^{0.5}$$

with d the bubble diameter, κ the polytropic exponent (~ratio of specific heats), ρ the gas density and P_o the ambient pressure. The dominant frequency observed on Earth in the oceans during periods of moderate rainfall (Scrimger, 1985) is ~13.5kHz, corresponding to a bubble size of 0.5mm.

Taking the same bubble size and imposing Titan conditions gives a frequency of ~20kHz, interstingly withing the API-S passband. However, as suggested in the following chapter, rainfall is unlikely to be heavy on Titan's oceans. Spilling breakers could be another source of bubbles, however.

The presence of large quantities of bubbles in liquids on Titan may be inferred from the liquid's density, it's reflectivity (measured by DISR) and turbidity (inferred from SSP REF external illumination measurement). Large numbers of bubbles with natural frequencies within the API passband are likely to make ocean depth measurement difficult - both due to increased ambient noise, and enhanced scattering of the sonar signal. On the other hand, detection of bubbles would be interesting for understanding atmosphere-ocean coupling on Titan.

References

Abbiss C P, Knobler C M, Teague R K and Pings C J, Refractive Index and Lorentz-Lorenz Function for Saturated Argon, Methane and Carbon Tetrafluoride, *J. Chem. Phys.* vol.42 pp.4145-4147, 1965

Achtermann E, Kapp R and Lehra H, Parachute Characteristics of Titan Descent Modules, ESA CR(P)2438, February 1986

Aerospatiale , Huygens Hardware Design Report, HUY-AS/c-100-RP-0180 (NB Project Document - circulation may be restricted) 1994

Allison M A, An Assessment of Titan's Boundary Layer, Symposium on Titan, Toulouse, September 1991 *ESA SP-338* pp.113-118, 1992

Atkinson D H, Pollack J B and Seiff A, Measurement of a Zonal Wind Profile by Doppler Tracking Cassini Entry Probe, *Radio Science* vol.25 pp.865-881, 1990

Badoz J, Nahoum R, Israel G and Raulin F, Experimental Determination of the Refractive Index of Liquified Gas Mixtures. Applications to Hypothesized Titan Oceans, *ESA SP-338*, pp.303-305, 1992

Baines K H , Brown R M, Matson D L, Nelson R M, Buratti B J, Bibring J-P, Langevin Y, Sotin C, Carusi A, Coradini A, Clark R N, Combes M, Drossart P, Sicardy B, Cruikshank D P, Formisano V and Jaumann R, VIMS/Cassini at Titan: Scientific Objectives and Observational Scenarios, ESA SP-338, pp.215-219, 1992

Balburnie C (producer), Design for An Alien World, programme TV5 in S281 course 'Images of the Cosmos', BBC Televison, Milton Keynes, 1994

Beckman J and Scoon G E N, Project Cassini - A Potential Collaborative ESA/NASA Saturn Orbiter and Titan Probe Mission, IAF-85-396, also published in *Acta Astronautica*, Vol.14 pp.185-194, 1986

Birchley, P N W, Development of a Refractometer and Thermal Properties Instrument for the Cassini Mission, PhD Thesis, University of Kent, 1992

Birchley P N W, Daniell P M, Zarnecki J C, Parker D J, Laboratory Determination of the Thermal Conductivity of Liquid Methane and Ethane, *ESA SP-338*, pp.311-314, 1992

Birchley P N W, Wright M J, Zarnecki J C, Ratcliff P R and Mill C S, Laboratory Determination of the refractive indices of Liquid Methane and Ethane at Temperatures Appropriate to the Surface of Titan, *ESA SP-338*, pp.307-310, 1992

Blamont J, A Method of Exploration of the Atmosphere of Titan, in D M Hunten and D Morrison (eds), The Saturn System, NASA CP-2068, 1978

Borucki W J and Fulchignoni M, Huygens-ASI Capabilities for Aerosol Measurements, in *ESA SP-338*, 1992

Broadfoot A L, Sandel B R, Shemansky D E, Holberg J B, Smith G R, Strobel D F, McConnell J C, Kumar S, Hunten D M, Atreya S K, Donahue T M, Moos H W, Bertaux J L, Blamont J E, Pomphrey R B, Linick S, Extreme Ultraviolet Observations from Voyager 1 Encounter with Saturn, *Science*, vol.212 pp.206-211, 1981

Broch J T, Acoustical Sensors for the Huygens Probe - The Acoustic Altimeter, Sintef/Delab report STF40 F91179, December 1991

Brown G S, The Average Impulse Response of a Rough Surface and Its Applications, *IEEE Transactions on Antennas and Propagation* AP-25, pp.67-74, 1977

Budden N A, Spudis P D, Evaluating Science Return in Space Exploration Initiative Architectures, NASA Tech. Paper 3379, 1993

Calcutt S, Taylor F, Ade P, Kunde V and Jennings D, The Composite Infrared Spectrometer, *Journal of the British Interplanetary Society*, vol.45 pp.811-816, 1992

Caldwell J , Cunningham C C, Anthony D, White H P, Groth E J, Hasan H, Noll K , Smith P H, Tomasko M G and Weaver H A, Titan: Evidence for Seasonal Change - A Comparison of HST and Voyager Images, *Icarus*, v.97 pp.1-9, 1992

Castelli A and Cornaro C, A Temperature Sensor for the Cassini/Huygens Probe, ASI Science meeting, Paris March 7-8, 1991

Castro A J, Titan Probe Technology Assessment and Technology Development Plan Study, NASA CR-152381, 1980

Chicarro A F, Coradini M, Fulchignoni M, Liede I, Lognonne P, Knudsen J M, Scoon G E N, Wanke H, Marsnet Assessment Study Report, ESA SCI(91)6, 1991

Ciarlo A and Schilling K, Application of Expert System Techniques to the Cassini Titan Probe, *ESA Journal* vol.12, pp.337-351

Clarke A C, Imperial Earth, Victor Gollancz, London, 1975

Collar P G, Packwood A R and Blane D D, Autosub - The NERC Community Research Project to Develop Autonomous Underwater Vehicles for Marine Science in the Deep Ocean, in proceedings of Oceanology Technology '90, Brighton, March 1990

Comoretto G, Bertotti B, Iess L and Ambrosini R, Doppler Experiments with the Cassini Radio System, *Il Nuovo Cimento*, vol.15C pp.1193-1198, 1992

Coustenis A , Spatial Variations of Temperature and Composition in Titans Atmosphere: Recent Results *Annales Geophysicae* vol.8 p.645-652, 1990

Coustenis A, Bezard B and Gautier D, Titan's atmosphere from Voyager Infrared observations. I. The gas composition of Titan's equatorial region, *Icarus*, vol.80, pp. 54-76, 1989

Coustenis A, Bezard B and Gautier D, Titan's Atmosphere from Voyager 1 Infrared Observations II. The CH_3D Abundance and D/H Ratio from the 900-1200 cm^{-1} Spectral Region, *Icarus* vol.82, pp.67-80, 1989

Coustenis A, Lellouch E, Maillard J P and McKay C P, Titan's Surface: Composition and Variability from the Near Infrared Albedo, Icarus (submitted) 1994

Coustenis A, Schmitt B, Samuelson R E and Khanna R K, Water Ice and Other Condensates in Titan's Stratosphere, submitted, 1994

Coustenis A,Bezard B, Gautier D and Marten A, Titan's Atmosphere from Voyager 1 Infrared Observations III. Vertical Distributions of Hydrocarbons and Nitriles near Titan's North Pole, *Icarus* vol.89, pp.152-167, 1991

Croft T A, Surface Reflections of Pioneer Venus Probe Radio Signals, *Geophysics Research Letters*, vol.7 pp.521-524, 1980

Cruikshank D P, The Development of Studies of Venus, in D M Hunten et al. (eds) Venus, University of Arizona Press, 1983

Desch M D and Kaiser M L , Upper Limit Set on Level of Lightning Activity on Titan, *Nature*, vol.343, pp.442-444,, 1990

Dorrington G E, Development of Human Powered Airships at Southampton 1991-1993, International Airship Conference , Stuttgart, Germany, June 1990

Dubouloz N, Raulin F,Lellouch E and Gautier D, Titan's Hypothesized Ocean Properties: The influence of Surface Temperature and Atmospheric Composition Uncertainties' *Icarus* 82 pp.81-96, 1989

Elachi C , Eastwood I M , Roth V L and Werner C L , Cassini Titan Radar Mapper, *Proceedings of the IEEE* vol.79 pp.867-879, 1991

English M A, Lara L M, Lorenz R D, Ratcliff P R and Rodrigo R, Ablation and Chemistry of Meteoric Materials in the Atmosphere of Titan, *Advances in Space Research*, submitted, 1994

ESA, Proposal to Place a Contract, ESA/IPC(90)129, 30 October 1990

ESA, Cassini Mission : Huygens Probe. Announcement of Opportunity, ESA SCI(89)2, October 1989

Eshleman V R , Radar Glory from Buried Craters on Icy Moons, *Science* vol.234 pp.587-590, 1986

Eshleman V R, The Radar-Glory Theory for Icy Moons with Implications for Radar Mapping, *Advances in Space Research* vol.7 No.5 pp.(5)133-(5)136, 1987

Eshleman V R, Lindal G F andTyler G L, Is Titan Wet or Dry, *Science* vol.221 pp.53-55, 1983

Fabris M, Marzari F, and Vanzani V, Titan's Atmospheric Structure from Huygens-ASI Measurements, *ESA SP-338*, pp.339-342, 1992

Farinella P, Paolicchi P , Strom R G, Kargel J S and Zappala V, The Fate of Hyperion's Fragments, *Icarus* vol 83 pp.186-204, 1990

Flasar F M, Oceans on Titan, *Science* vol.221 pp.55-57,1983

Flasar F M and Conrath B J , Titan's Stratospheric Temperatures: A Case for Dynamic Inertia?, *Icarus* vol.85, pp.346-354, 1990

Flasar F M, Samuelson R E and Conrath B J , Titans Atmosphere: temperature and dynamics, *Nature* vol.292 pp.693-698, 1981

Formisano V, Adriani A and Bellucci G, The VNIR-VIMS Experiment for CRAF-Cassini, *Il Nuovo Cimento*, vol.15C, pp.1179-1192, 1992

Friedlander A L, Titan Buoyant Station, *J. Brit. Interplan. Soc.*, v.37, pp.381-387, 19841959

Friedlander A L, Buoyant station Mission Concepts for Titan Exploration, IAF-85-417, 1985

Froidevaux F and Ingersoll A P, Temperatures and Optical Depths of Saturn's Rings and a Brightness Temperature for Titan, *Journal of Geophysical Research*, vol.85 pp.5929-5936

Fulchignoni M, The Atmosphere of Titan and the Huygens Atmospheric Structure Instrument, *Il Nuovo Cimento* vol.15C pp.1163-1177, 1992

Furlong R, Cassini RTG Program: Cassini Project Review, in Cassini Project Mission and Spacecraft system delta preliminary design review (D-PDR), JPL 1699-0135, 1992

Geake J E and Firth C S, The Huygens SSP Refractometer, *ESA SP-338*, pp.343-346, 1992

Gibbons A, Has Challenger knocked out Galileo?, *Science* vol.253 pp.846-847, 1991

Goldstein R M and Green R R, Ganymede: Radar Surface Characteristics, *Science* vol.207, pp.179-180, 1980

Grard R J L, The significance of Meteroic Ionisation for the Propagation of Lightning Spherics in the Atmosphere of Titan, *ESA SP-338* pp.125-128, 1992

Grard R J L, A quadrupolar array for measuring the complex permitivity of the ground: application to Earth prospection and planetary exploration, *Measurement Science and Technology*, vol.1 pp.295-301, 1990a

Grard R J L, A quadrupole system for measuring in situ the complex permittivity of materials: application to penetrators and landers for planetary exploration, *Measurement Science and Technology*, vol.1 pp.801-806, 1990b

Grard R J L, Svedhem H, Brown V, Falkner P and Hamelin M , An Experimental Investigation of Atmospheric Electricity and Lightnign Activity during the Descent of the Huygens Probe on Titan, submitted 1993

Greeley R, Planetary Landscapes, Unwin Publishers, Winchester USA, p.66, 1987

Griffith C A, Evidence for surface heterogeneity on Titan, *Nature* vol.364 pp.511-514 , 1993

Griffith C A and Owen T C, Observing the Surface of Titan through Near-Infrared Windows in its Atmosphere, *ESA SP-338*, pp.199-204, 1992

Griffith C A, Owen T and Wagener R, Titans Surface and Troposphere, Investigated with Ground-Based, Near-Infrared Observations, *Icarus* 93 pp.362-378, 1991

Grossman A W and Muhleman D O, Observations of Titan's Radio Light-Curve at 3.5cm., (abstract) *Bull. Amer. Astron. Soc.* vol.24 No 3 p.954, 1992

Grundy W, Lemmon M, Fink U, Smith P and Tomasko M, Windows Through Titan's Atmosphere, (abstract) *Bulletin of the American Astronomical Society* vol.23 p.1186, 1991

Gurnett D A, Grun E, Gallagher D, Kurth W S and Scarf F L, Micron-sized particles detected near Saturn by the Voyager plasma wave instrument, *Icarus*, vol.53, p.236 ,1983

Gurrola E M and Eshleman V R, On the Angle and Wavelength dependencies of the radar backscatter from the icy Galilean moons of Jupiter, *Advances in Space Research* vol.10 No.1 pp.(1)195-(1)198, 1990

Hagfors T, Gold T and Ieric H M, Refraction Scattering as origin of the anomalous radar returns of Jupiter's Satellites, *Nature* vol.315, p.637-640, 1985

Hanel R , Conrath B, Flasar F M, Kunde V, Maguire W, Pearl J, Pirraglia J, Samuelson R, Herath L, Allison, M, Cruikshank D, Gautier D, Gierasch P, Horn L, Koppany R, and

Ponnamperuma C, Infrared observations of the Saturnian system from Voyager 1, *Science* vol.212 pp.192-200, 1981

Hapke B and Blewett D , Coherent backscatter model for the unusual radar reflectivity of icy satellites, *Nature* v.352, pp.46-47, 1991

Hassan H, McCarthy C and Wyn-Roberts D, Huygens - A Technical and Programmatic Overview, *ESA Bulletin* 77, pp.21-30, 1994

Healy G J, Aircraft Far-Field Aerodynamic Noise: Its Measurement and Prediction, in I R Schwartz, H T Nagamatsu and W C Strahle (eds, Aeroacoustics: STOL noise; airfrane and airfoil noise, Vol.45 in Progress in Astronautics and Aeronautics, 1975

Hechler F, Cassini-Huygens Interplanetary Trajectories and Initial Orbits about Saturn, MAS Working Paper No.307, ESOC, 1990

Hill R D, Thunder, pp.385-406 in Golde R H (ed), Lightning, vol.1, Academic Press, 1977

Hubbard W B , Hunten D M, Reitsema H J, Brosch N, Nevo Y, Cerreira E, Rossi F and Wasserman L H,, Results for Titan's Atmosphere from its Occultation of 28 sagitarii, *Nature*, vol.342, pp.353-355, 1990

Hubbard W B, Sicardy B , Miles R, Hollis A J, Forrest R W, Nicolson I K M, Appleby G, Beisker W, Bittner C, Bode H-J, Bruns M, Dezau H, Nezel M, Riedel EE, Struckman H, Arlot J E, Roques F, Sevre F, Thuillot W, Hoffman M, Geyer E H, Buil C, Colas F, Lecacheux J, Klotz A, Thouvenot E, Vidal J L, Cerreira E, Rossi F, Blanco C, Cristaldi S, Nevo Y, ReistsemaH J, Brosch N, Cernis K, Zdanavicius K, Wasserman L H, Hunten D M, Gautier D, Lellouch E, Yelle R V, Rizk F, Flasar F M, Porco C C, Toublanc D and Corugedo G, The Occultation of 28-Sgr by Titan, *Astronomy and Astrophysics* vol.269, No.1-2 pp.541-563, 1993

Humes D H, Results of Pioneer 10 and 11 Meteoroid Experiments: Interplanetary and Near-Saturn, *Journal of Geophysical Research*, vol.85 No.A11 pp.5841-5852, 1980

Hunten D M, The Atmosphere of Titan, NASA SP-340, 1974

Hunten D M, A Titan Atmosphere with a Surface Temperature of 200K, in The Saturn System, NASA CP 2068, pp.127-140, 1978

Hunten D M, The Thermal Structure of the Atmopshere of Titan, Proceedings of the Symposium on Titan, Toulouse September 1991 (*ESA SP-338*) pp.37-40, 1992

Hunten D M, Tomasko M G, Flasar F M, Samuelson R E, Strobel D F and Stevenson D J, Titan in Gehrels and Matthews (eds) Saturn, University of Arizona Press, Tucson, 1984

Huygens C , De Saturnii Luna Observatio Nova, March 1656

Huygens C, The Celestial Worlds Discover'd, 1698

Ip W H, **Gautier D et al.,** Project Cassini: A Proposal to the European Space Agency for a Saturn Orbiter/Titan Probe Mission, 15th November 1982

Isbell D, Budget Alarms Scientists, *Space News* vol.3 No.5 February 10-16, 1992

Israel G, Chassefiere E, Niemann H B, Boon J J, Muller C, Raulin F, Cabane M, and Sable C, Huygens/ACP: An Instrument for Aerosols Chemical Composition Measurements, *ESA SP-338*, pp.225-228, 1992

Jaffe W, Caldwell J and Owen T, Radius and Brightness Temperature Observations of Titan Centimetre Wavelengths by the Very Large Array, *Astrophysical Journal*, v.242, pp.806-811 1980

Jeans J H , Dynamical Theory of Gases, 4th ed. pp.346-348, Cambridge 1925

Johnson T V and Gautier D, Saturn Orbiter/Titan Probe Mission, in Planetary Science in Euro European Science Foundation, 1992

Kamoun P , Anne J C and Ford P, ASTRA : Altimetry and Sounding of Titan with a radar on a descending craft, Proceedings International Symposium on Radars and Lidars in Earth and Planetary Sciences, Cannes, France 2-4 September, 1991 (*ESA SP-328*) pp.71-78 ,1992

Kim S J and Caldwell J , The abundance of CH_3D in the atmosphere of Titan, derived from 8- to 14-micron thermal emission, *Icarus* vol.52, 473-482, 1982

Kohlhase C, Meeting with a majestic Giant, *The Planetary Report* vol.13, July 1993

Kouvaris L C and Flasar F M, Phase Equilibrium of Methane and Nitrogen at Low Temperatures: Application to Titan, *Icarus* vol.91 pp.112-124, 1991

Ksanfomality L V, Scarf F L and TaylorW W L , The Electrical Activity of the Atmosphere Venus' in D M Hunten et al. (eds) 'Venus' University of Arizona , 1983a

Ksanfomality L V, Goroshkova N V and Khondryev V K, Wind Velocity Near the Surface c Venus form Acoustic Measurements, *Cosmic Research* vol.21 pp.161-167 (translated from *Kosmicheskii Issledovania* vol.21 pp.218-224), 1983b

Kuiper G P, Titan - A Satellite with an Atmosphere, *Astrophysical Journal*, vol.100 pp.378-383, 1944

Lara L M, Estudio Fotoquimico de los componentes neutros de la atmosfera de Tita, PhD Thes University of Granada, Spain, 1993

Lara L M, Lorenz R D and Rodrigo R, Liquids and Solids on the Surface of Titan, *Planetary a Space Science*, vol.42 pp.5-14, 1994 (Appendix 6)

Lebreton J-P , The Huygens Probe, Proceedings of the Symposium on Titan, Toulouse, 9-12 September 1991, *ESA SP-338* pp.287-292, 1992

Lebreton J-P and Matson D, Cassini - A Mission to Saturn and Titan, Proceedings of 24th ESL Symposium on the Formation of Stars and Planets and the Evolution of the Solar System, Freidrichshafen 17-19 September 1990 (*ESA SP-315*) pp.7-12, 1990

Lebreton J-P and Matson D L, An overview of the Cassini Mission, *Il Nuovo Cimento* vol.15C pp.1137-1147, 1992

Lebreton J-P and Scoon G E, Cassini - A Mission to Saturn and Titan, *ESA Bulletin* 55, pp.24-1988

Leigh B R, Using the Momentum Method to Estimate Aircraft Ditching Loads, *Canadian Aeronautics and Space Journal*, vol.24 pp.162-168, 1988

Lellouch E and Hunten D M, Titan Atmosphere Engineering Model, ESLAB 87/199, ESA Spa Science Department, 1987

Lellouch E, Hunten D M , Kockarts G and Coustenis A, Titan's Thermosphere Profile, *Icarus,* vol.83, pp.308-324, 1990

Lemmon M T, Karkoshka E and Tomasko M, Titans Rotation: Surface Feature Observed, *Icarus* vol.103 pp.329-332, 1993

Lemmon M T, Karkoshka E and Tomasko, M, Titan's Rotational Lightcurve, *Icarus* (submitted) 1994

Letourneur B and Coustenis A, Titan's Atmosphere from Voyager 2 Infrared Spectra, *Planetary and Space Science,* vol.41 pp.593-602, 1993

Lewis J S, Satellites of the Outer Planets: Their Physical and Chemical Nature, *Icarus* vol.15 pp.174-185, 1971

Li M and Vitanyi P, An Introduction to Kolmogorov Complexity and Its Applications, Springer-Verlag, New York, 1993

Lindal G F, Wood G E, Hotz H B, Sweetnam D N, Eshleman V R and Tyler G L, The Atmosphere of Titan: An analysis of the Voyager 1 Radio Occultation Measurements, *Icarus,* vol.53, pp.348-363, 1983

Lingard J S and Underwood J C, Wind Tunnel Testing of Disk-Gap-Band Parachutes Related to the Cassini-Huygens Mission, RAeS/AIAA Aerodynamic Decelerator Systems Technology Conference, AIAA-93-1200, London, May 1993

Lorenz R D, The Huygens Mission to Titan, Estec Internal Working Paper EWP-1628, September 1991

Lorenz R D, Huygens Probe - The Surface Mission, Symposium on Titan, Toulouse, September 1991, *ESA SP-338* pp.359-364, 1992a

Lorenz R D, Gravitational Tide in the Atmosphere of Titan, Proceedings of the Symposium on Titan, Toulouse, September 1991 (*ESA SP-338*) pp.119-123, 1992b

Lorenz R D, Wake-Induced Dust Cloud Formation following Impact of Planetary Landers, *Icarus* vol.101 pp. 165-167, 1993a (Appendix 3)

Lorenz R D, Scientific Implicationd of the Huygens Probe Parachute System, AIAA-93-1215, 12th RAeS/AIAA Aerodynamic Decelerator Systems Technology Conference, London, May 1993b

Lorenz R D, The Life, Death and Afterlife of a Raindrop on Titan, *Planetary and Space Science,* vol.41 pp.647-655, 1993c (Appendix 4)

Lorenz R D, The Surface of Titan in the Context of ESA's Huygens Probe, *ESA Journal* vol.17 pp.275-292, 1993d (Appendix 5)

Lorenz R D, Huygens Probe Impact Dynamics, *ESA Journal* vol.18 pp.93-117, 1994a (Appendix 8)

Lorenz R D, Crater Lakes on Titan: rings, horseshoes and bullseyes, *Planetary and Space Science,* vol.42 pp.1-4, 1994 b (Appendix 9)

Lorenz R D, Raindrops on Titan, *Advances in Space Research* , vol.15 pp.(3)317-(3)320, 1995

Lorenz R D, Bannister M, Daniell P M, Krysinski Z, Leese M R, Miller R J, Newton G, Rabbets P and Willett D M , An impact penetrometer for a landing spacecraft, *Measurement Science and Technology*, vol.5 pp.1033-1041, 1994 (Appendix 7)

Lorenz R D and Svedhem L H, Acoustic Environment on Titan, poster presented at EGS Conference, Edinburgh, April 1992 (Abstract in *Annales Geophysicae*, vol.10, Supplement No.3, p.C487)

Lorenz R D and Zarnecki J C , Precipitation on Titan and the Methane Icing Hazard to the Huygens Probe, Presented at the European Geophysical Society, Edinburgh, Scotland, April 1992 (Abstract in *Annales Geophysicae*, vol.10, Supplement No.3, p.C487)

Low F Jand Rieke G H, Infrared Photometry of Titan, *Astrophysical Journal*, vol.190 pp.L143-145, 1974

Lucey P G and Clarke R N, Spectral Properties of Water Ice and Contaminants, in J Klinger et al. (eds) Ices in the Solar System, p.155-168, D Reidel Publishing Co. 1985

Lunine J I, Titan's Surface: Nature and Implications for Cassini, in The Atmospheres of Saturn and Titan, *ESA SP-241*, 1985

Lunine J I, Origin and Evolution of Outer Solar System Atmospheres, *Science* vol.241 pp.141-147, 1989

Lunine J I, The Urey Prize Lecture: Volatile Processes in the Outer Solar System, *Icarus*, vol.81, pp.1-13, 1989b

Lunine,J I, Evolution of the Atmosphere and Surface of Titan, *ESA SP-315*, pp.159-165, 1990

Lunine J I, Plausible Surface Models of Titan, *ESA SP-338* pp.233-239, 1992

Lunine, J I, Does Titan Have an Ocean? A Review of Current Understanding of Titans Surface, *Reviews of Geophysics* vol.31 pp.131-149, 1993

Lunine, J I, Does Titan Have Oceans, *American Scientist*, vol.82, pp.134-143, 1994

Lunine J I and Rizk B, Thermal Evolution of Titan's Atmosphere, *Icarus* vol.80, pp.370-389, 1989

Lunine J I and Stevenson D J, Evolution of Titan's Coupled Ocean-Atmosphere System and Interaction of Ocean with Bedrock, in J Klinger et al. (eds), Ices in the Solar System, pp.741-757, Reidel, 1985

Lunine J I and Stevenson D J, Clathrate and Ammonia hydrates at high pressure : Application to the Origin of Methane on Titan, *Icarus* vol.70 pp. 61-77, 1987

Lunine J I, Stevenson D J and Yung,Y L, Ethane Ocean on Titan, *Science* vol.222 pp. 1229-1230, 1983

Lutz B L , DeBergh C and Owen T , Titan: discovery of carbon monoxide in its atmosphere' *Science*, v.220 pp.1374-1375, 1983

Maeda H, Umeda Y and Arihara N, An Ultrasonic Altitude-Velocity Sensor for Airplanes in the Vicinity of the Ground, *Memoirs of the Faculty of Engineering*, Kyoto University vol.32 pp.249-259, 1970

Martin-Marietta, A Titan exploration Study - Science, Technology, and Mission Planning Options (vol.2), NASA-CR-137847, 1976

McCarty J L, Beswick A G and Brooks G W, Application of Penetrometers to the Study of Physical Properties of Lunar and Planetary Surfaces, NASA TN D-2413, 1964

McCarty J L and Carden H D, Impact Characteristics of Various Materials Obtained by an Acceleration-Time-History Technique Applicable to Evaluating Remote Targets, NASA TN D-1269, 1967

McCartney B S, and Collar P G, Autonomous Submersibles - Instrument Platforms of the Future, *Underwater Technology*, vol.15 pp.19-25, 1990

McDonald G D, Thompson W R, Heinrich M, Khare B N and Sagan C, Chemical Investigation of Titan and Triton Tholins, *Icarus*, vol.108 pp.137-145, 1994

McKay C P, Pollack J B and Courtin R, The Thermal Structure of Titan's Atmosphere, *Icarus* vol.80, pp.23-53, 1989

McKay C P, Pollack J B, Lunine J I and Courtin R, Coupled Atmosphere-Ocean Models of Titan's Past, *Icarus*, vol.102, pp.88-98, 1993

Minnaert M, On Musical Air-Bubbles and the Sounds of Running Water, *The London, Edinburgh and Dublin Philosophical Magazine and Journal of Science* vol.16, pp.235-248, 1933

Mitchell B J, Conceptual Design of a modified XBT Telemetry System for Use in the Oceans of Titan, submitted to International Telemetry Conference, 1994

Mooij E, De Cassini-missie, *Ruimtevaart* June 1992 pp.2-8, 1992

Mordaunt D H, Lambert I R, Morley G P, Ashfold M N R, Dixon R N, Western C M, Schneider L and Welge K H, Primary product channels in the photodissociation of methane at 121.6nm, *J. Chem. Phys*, vol.98, pp2054-2065, 1993

Muhleman D O, Grossman A W, Butler B J and Slade M A, Radar Reflectivity of Titan, *Science* vol.248 pp.975-980, 1990

Muhleman D O, Grossman A W , Slade M A and Butler B J, The Surface of Titan and Titan's Rotation: What is Radar Telling Us?, *Bull. Amer. Astron. Soc.* vol.24 No.3, 1992

Muhleman D O, Grossman A W, Slade M A and Butler B J, Titan's Radar Reflectivity and Rotation, *Bulletin of the American Astronomical Society*, vol. 25, p1099, 1993

Murphy J P, Cuzzi J N, Butts A J, and Carroll P C, Entry and Landing Probe for Titan, *J. Spacecraft and Rockets*, vol.8 pp.157-163, 1981

Murray C D, The Cassini Imaging Science Experiment, *Journal of the British Interplanetary Society*, vol.45 pp.359-364, 1992

Murrow D W, Cassini Mission Plan, PD 699-100-2 rev B, JPL, May 1993

NASA/ESA , Cassini - Saturn orbiter and Titan Probe, ESA/NASA Assessment Study, ESA SCI(85)1, August 1985

NASA/ESA, Cassini, Supplement to the Assessment Study, ESA SCI(86)5, December 1986

NASA/ESA, Cassini Phase A study ESA/SCI 88(5)

Neal M F andWellings P J, Descent Control Subsystem for the Huygens Probe, !2th RAeS/AIAA Aerodynamic Decelerator Systems Technology Conference, AIAA-93-1221, London, May 1993

Nelson H F, Park C and Whiting E E, Titan Atmospheric Composition by Hypervelocity Shc Layer Analysis, AIAA 24th Thermophysics Conference, AIAA-89-1770, Buffalo, June 1989

Ness N F, Acuna M H, Lepping R P, Connery J E P, Behannon K W abd Burlaga L F, Magnetic Field Studies by Voyager 1: Preliminary Results at Saturn, *Science*, vol.212 pp. 211-217, 1981

Newton G P, Cassini Mission Project Penetrometer, Final Year Project Report (Physics with Computing) University of Kent, 1994

Noll K S and Knacke R F, Titan: 1-5um photometry and spectrophotometry and a search for variability, *Icarus* vol.101 pp.272-281, 1993

Oberbeck V R, O'Hara D and Carle G C, Concepts for Collection of Aerosols in Titan's Atmosphere, *Journal of Geophysical Research*, vol.92 No.B4 pp.E717-E722, 1987

Ostro S J, Campbell D B, Simpson R A, Hudson R S, Chandler J F, Rosema K D, Shapiro I I, Standish E M, Winkler R, Yeomans D K, Velez R and Goldstein R M, Europa, Ganymede, anc Callisto: New Radar Results From Arecibo and Goldstone, *Journal of Geophysical Research*, vol.97 No.E11 pp.18,227-18,244, 1992

Ott S, Analysis of the Targeting Requirements for the Huygens Mission, Estec Internal Work Paper EWP-1640, December 1991

Ott S, Cassini Mission : The Targetting of the Huygens Probe, IAF-92-0067 Presented at the World Space Congress, Washington DC, September 1992

Owen T, How Primitive are the Gases in Titan's Atmosphere, *Advances in Space Research*, vol.7 pp.51-54, 1987

Owen T and Gautier D, Titan: Some New Results, *Advances in Space Research*, vol.9 pp.(2)7 (2)78, 1989

Peale S J, Cassen P and Reynolds R T, Tidal Dissipation, Orbital Evolution and the Nature Titan's Inner Satellites. *Icarus* 43 pp.65-72, 1980

Picardi G, Seu R , Coradini A, Zampolini E and Ciaffone A, The Radar System for the Exploration of Titan, *Il Nuovo Cimento*, vol.15C pp.1149-1161, 1992

Pinto J P, Lunine J I, Kim S J and Yung Y L, D to H ratio and the origin and evolution of Titan's Atmosphere, *Nature* vol.319, pp.388-390, 1986

Pouliquen M, 1992, Space Transportation Systems, Presentation at International Space University (Engineering Department) Summer Session, Kitakyushu, Japan.

Pollack J B, Atkinson D H, Seiff A and Anderson J D, Retreival of a Wind Profile from the Galileo Probe Signal, *Space Science Reviews*, vol.60 pp.143-178, 1992

Powell G, Schurmeier B and Murray B, Measuring Speed on the Mars-96 balloon guiderope System, IAF-93-U.6.585, presented at 44th International Astronautical Federation Congress Graz, Austria, October 1993

Prange R, The Cassini Mission - Complementary Observations with the Space Telescope, in The Atmospheres of Saturn and Titan, *ESA SP-241*, pp.209-217, 1985

R O Fimmel, L Colin and E Burgess, Pioneer Venus, *NASA SP-461* , 1983

Rapley C, Satellite Radar Altimeters, in R A Vaughan (ed), Microwave Remote Sensing for Oceanographic and Marine Weather-Forecast Models, pp.45-63, Kluwer Academic Presss, 1990

Raulin F, Accaoui B, Razaghi A, Dang-Nhu M, Coustenis A and Gautier D, Infrared Spectra of gaseous organics : Application to the atmosphere of Titan - II. Infrared intensities and frequencies of C4 alkenenitriles and benzene, *Spectrochemica Acta* vol.46A, pp.671-683, 1990

Raulin F, Frere C, Paillous P, de Vanssay E, Po L and Khlifi M, Titan and the Exobiological Aspects of the Cassini/Huygens Mission, *Journal of the British Interplanetary Society* vol.45 pp.257-271, 1992

Rebiai R , Rest A J and Scurlock R G, The Unexpectedly High Solubility of Water in Cryogenic Liquids, *Nature* vol.305 pp.412-413, 1983

Rest A J , Scurlock R G and Wu M F, The Solubilities of Nitrous Oxide, Carbon Dioxide, Aliphatic Ethers and Alcohols, and Water in Cryogenic Liquids, *The Chemical Engineering Journal* vol.43 pp.25-31, 1990

Ringwood S D, Looking over Galileo's Shoulder, *Astronomy Now*, vol.8 No.4 , pp.48-52, 1994

Rock W, Auweter-Kurtz M, Dabal P, Fruholz H, Habiger H and S Laure, Experimental Simulation of the Entry of Huygens into the Titan Atmosphere for the Thermal Protection Qualification, IAF-93-I.3.227, IAF Congress, Graz, Austria, October 1993

Rothery D A and Lawrence G, Remote Sensing for the Study of Volcanoes and Earthquakes, *Geoscientist*, vol.3 No.6, 1993

Sable C and Villaeys J, Choix des Materiaux d'enveloppe pour vehicules d'exploration planetaire (Venus-Mars-Titan), in Materials in the Space Environment, *ESA SP-178*, 1982

Sagan C, Structure of the Lower Atmosphere of Venus, *Icarus*, vol.1, pp.151-169, 1962

Sagan C and S F Dermott, The Tide in the Seas of Titan. *Nature* vol. 300 pp.731-733, 1982

SAIC, Titan Exploration with Advanced Systems, a study of future mission concepts, NASA-CR-173499, 1983

Sainct H and Clausen K, Technologies New to Space in Huygens Probe Mission to Titan, IAF-93-U.4.564, Presented at 44th IAF Congress, Graz, Austria, October 1993

Saint-Pe O, Combes M, Rigaut F, Tomasko M and Fulchignoni M, Demonstration of Adaptive Optics for Resolved Imagery of Solar System Objects: Preliminary Results on Pallas and Titan,*Icarus* vol 105, 263-270, 1993

Samuelson R E, Cassini/CIRS Capabilities for Aerosol, Cloud and Surface Measurements, *ESA SP-338*, pp.221-214, 1992

Samuelson R E , Hanel R A, Kunde V G and Maguire W C, Mean Molecular Weight and Hydrogen Abundance of Titan's Atmosphere, *Nature*, vol.292, pp.688-693, 1981

Schmitt B, Quirico E and Lellouch E, Near Infrared Spectra of Potential Solids at the Surface of Titan, *ESA SP-338* pp.383-388, 1992

Schock A, Effect of Mode-Switching on Output of Mariner/Mark-2 RTGs, IAF-92-0571, 43rd IAF Congress, Washington DC, September 1992

Scoon G E , Cassini - A Concept for a Titan Probe, *ESA Bulletin* 41, pp.12-20, 1985

Scoon G, Whitcomb G, Eiden M, and Smith A, Cassini Huygens Entry and Descent Technologi IAF-89-028, presented at 40th IAF Congress, Malaga, Spain, October 1989

Scrimger J A, Underwater Noise Produced by Precipitation, *Nature* vol.318 pp.647-649, 1985

Sears W, A Numerical model of Tidal Dissipation on Titan, *Icarus*,(submitted) 1994

Sears W, Lunine J I and Greenberg R, Equilibrium Nonsynchronous Rotation of Titan, *Icarus*, v.105 pp.247-252, 1993

Seiff A, The Viking Atmosphere Structure Experiment - Techniques, Instruments, and Expecte Accuracies, *Space Science Instrumentation*, vol.2 pp.381-423, 1976

Seiff A, Atmospheres of Earth, Mars and Venus, as Defined by Entry Probe Experiments, *J. Spacecraft and Rockets*, vol.28 pp.265-275, 1991

Seiff A, Juergens D W and Lepetich J E, Atmospheric Structure Instruments on the Four Pionee Venus Entry Probes, *IEEE Transactions on Geoscience and Remote Sensing*, vol. GE-14, pp.1105 11, 1980

Seiff A and Knight T C D, The Galileo Probe Atmospheric Structure Instrument, *Space Scien Reviews*, vol.60, pp.203-232, 1992

Sicardy B, Brahic A, Ferrari C, Gautier D, Lecacheux J, Lellouch E, Roques F, Arlot J E, Colas Thuillot W, Sevre F, Vidal J L, Blanco C, Cristaldi S, Buil C, Klotz A and Thouvenot E, Probing Titan's Atmosphere by Stellar Occultation, *Nature*, vol.342 pp.350-353, 1990

Smith B A , Soderblom L, Beebe R, Boyce J, Briggs G, Bunker A, Collins S A, Hansen C J, Johns T V, Mitchell J L, Terrile R J, Carr M, Cook A F II, Cuzzi J, Pollack J B, Danielson G E, Ingerso A, Davies M E, Hunt G E, Masursky H, Shoemaker E, Morrison D, Owen T, Sagan C, Veverka Strom R and Suomi V E, Encounter with Saturn: Voyager 1 Imaging Science Results, *Science* vol.212 pp.163-191, 1981

Smith K, Titan Probe Options: A study of Future Mission Concepts, B.Eng. Honours report, Department of Aeronautics and Astronautics, University of Southampton, May 1993

Smith P H, The Radius of Titan from Pioneer Saturn Data, *Journal of Geophysical Research*, vol.85 No.A11 pp.3943-3947

Smith P and Lemmon M, HST Images of Titan, (abstract) *Bulletin of the American Astronomical Society* vol.25 p.1105, 1993.

Sohl F, Sears W, and Lorenz R D, Tidal Dissipation on Titan, *Icarus* (submitted July 1994)

Sperling F and Galba J A, Treatise on the Surveyor Lunar Landing Dynamics and an Evaluat of Pertinent Telemetry Data Returned by Surveyor 1' Technical Report 32-1035, Jet Propulsio Laboratory, 1967

Srokosz M A, Challenor P G, Zarnecki J C and Green S F, Waves on Titan, *ESA SP-338*, pp.32 323, 1992

Sromovsky L A, Suomi V E, Pollack J B, Krauss R J, Limaye S S, Owen T, Revercomb H E, Sag C, Implications of Titan's North-South Brightness Assymetry, *Nature* vol.292, pp.698-702, 1981

Stammes P, The detectability of Titans Surface in the Near-Infrared, *ESA SP-338* pp.205-21 1992

Stevenson D J, Interior of Titan. Proceeedings of the Symposium on Titan, Toulouse, September 1991 (*ESA SP-338*) pp.29-33, 1992

Stevenson D J and Potter B E, Titan's Latitudinal Temperature Distribution and Seasonal Cycle. *Geophysical Research Letters* vol.13 pp.93-96, 1986

Strobel D F , Hall D T, Zhu X and Summers M E, Upper Limit on Titan Atmospheric Argon abundance, *Icarus* vol.103, pp.333-336, 1993

Stubbs S M, Dynamic Model Investigation of Water Pressures and Accelerations Encountered during Landings of the Apollo Spacecraft, NASA TN D-3980, 1967

Szabo N, Measuring Scientific Value, article 5272 on Usenet newsgroup sci.research, 1994

Tanguy L , Bezard B, Marten A, Gautier D, Gerard E , Paubert G and Lecacheaux A, Stratospheric profile of HCN on Titan from Millimetre observations, *Icarus* vol.85 pp.43-57, 1990

Thompson W R and Sagan C, Far IR and Microwave Remote Sensing of Titan's Methane Clouds and Organic Haze, *Icarus* vol.59, pp.133-161, 1984

Thompson W R and Sagan C, Organic Chemistry on Titan - Surface Interactions, Symposium on Titan, Toulouse, September 1991 *ESA SP-338* pp.167-176, 1992

Thompson W R and Squyres S W , Titan and other Icy Satellites - Dielectric Properties of Constituent Materials and Implications for radar Sounding, *Icarus* vol.86 pp.336-354, 1990

Thompson W R, Zollweg J A and Gabis D H, Vapor-Liquid Equilibrium Thermodynamics of N_2+CH_4: Model and Titan Applications, *Icarus* vol.97 pp.187-199, 1992

Tomasko, M G, Preliminary Results of Polarimetry and Photometry at large Phase Angles from Pioneer 11, *Journal of Geophysical Research*, vol.85 No.A11 pp.5937-5942

Toon O B, McKay C P , Courtin R and Ackerman T P, Methane Rain on Titan, *Icarus* vol.75 pp.255-284, 1988

Toon O B, Mckay C P, Griffith C A and Turco R P , A Physical Model of Titan's Aerosols, *Icarus* vol. 95, pp.24-53, 1992

Tyler G L, Eshleman V R, Anderson J D, Levy G S, Lindal G F, Wood G E and Croft T A, Radio Science Investigations of the Saturn System with Voyager 1: Preliminary Results, *Science* vol.221, pp.201-206, 1981

Ulamec S, Stagiaire Report, ESTEC 1987

Ulamec S, Possible Applications for an Acoustic Instrument aboard the Huygens Probe, ESTEC Internal Report, 1990

Ulamec S, Badoz J and Lebreton J-P, Dielectric Constant Measurements in Simulated Titan Ocean Liquids, *ESA SP-338*, pp.401-405, 1992

Ulamec S and Svedhem L H, Reflection of Acoustic Pulses from a Simulated Titan Liquid Surface, unpublished note 1992

Van Helden A , Saturn through the Telsecope : A Brief Historical Survey, in T Gehrels and M S Matthews (eds), Saturn, University of Arizona Press, pp.23-43, 1984

Van Loef J J, On the Thermal Conductivity of Methane-Ethane Mixtures, *Physica B*, vol.141, pp.213-215, 1986

Velazquez A, Huot J-P and Molina R C, Aerothermodynamics Effects during the Huygens Entry Phase, Symposium on Aerothermodynamics for Space Vehicles (*ESA SP-318* pp.61-66), July 1991

Webster C R, Stratospheric Composition Measurements of Earth and Titan using High-Resolution Tunable Diode Laser Spectroscopy, *J. Quant. Spectrosc. Radiat. Transfer*, vol.40 pp.239-248, 1988

Wenkert D D and Garneau G W, Does Titan's Atmosphere have a 2-day rotation period, (abstract) *Bulletin of the American Astronomical Society* vol.19 p.875, 1987

Wild W J and Fugate R Q, Untwinkling the Stars, *Sky and Telescope*, vol.87 No.6, pp.20-27, 1994

Willett D M, Calibration of Cassini SSP Penetrometer, Third Year Project Report, University of Kent, 1994

Wilson A, Solar System Log, Janes, London 1987

Young C W, The Development of Empirical Equations for Predicting Depth of an Earth-Penetrating Projectile, SC-DR-67-60, Sandia Labs, May 1967

Yung Y L, Allen M and Pinto J P, Photochemistry of the Atmosphere of Titan: comparison between model and observations, *Astrophysical Journal (Supplement Series)* vol.55 pp.465-506, 1984

Zahnle K, Pollack J B and Grinspoon D, Impact-Generated Atmospheres over Titan, Ganymede and Callisto. *Icarus* vol.95 pp.1-23, 1992

Zarnecki J C, Surface Science Package for the Huygens Titan Probe, *Journal of the British Interplanetary Society*, vol.45 pp.365-370, 1992

Zarnecki J C, McDonnell J A M, Green S F, Stevenson T J, Birchley P N W, Daniell P M, Niblett D H, Ratcliff P R, Shaw H A, Wright M J, Cruise A M, Delderfield J, Parker D J, Douglas G, Peskett S, Morris N, Geake J E, Mill C S, Challenor P G, Fulchignoni M, Grard R J L, Svedhem H, Clark B, Boynton W V, A Surface Science Package for the Huygens Titan Probe, *ESA SP-338*, pp.407-409, 1992

Zubrin R, Missions to Mars and the Moons of Jupiter and Saturn Utilizing Nuclear Thermal Rockets with Indigenous Propellants, AIAA-90-0002, 28th Aerospace Sciences Meeting, Reno, Nevada Januray 1990

Zubrin R, The Case for Titan, *Ad Astra*, pp.26-30, June 1991